



www.sciencemag.org/cgi/content/full/science.1249830/DC1

## Supplementary Material for

### **A bump-and-hole approach to engineer-controlled selectivity of BET bromodomain chemical probes**

Matthias G. J. Baud, Enrique Lin-Shiao, Teresa Cardote, Cynthia Tallant, Annica Pschibul, Kwok-Ho Chan, Michael Zengerle, Jordi R. Garcia, Terence T.-L. Kwan, Fleur M. Ferguson, Alessio Ciulli\*

\*Corresponding author. E-mail: a.ciulli@dundee.ac.uk

Published 16 October 2014 on *Science Express*  
DOI: 10.1126/science.1249830

**This PDF file includes:**

Materials and Methods

Supplementary Text

Figs. S1 to S11

Tables S1 to S6

Full Reference List

## Materials and Methods

### Plasmids and peptides

Plasmids pNIC28-Bsa4 Kan<sup>r</sup> containing the 8 single BET bromodomain constructs brd2(1) (protein start and stop positions K71-K176), brd2(2) G344-D455, brd3(1) P24-E144, brd3(2) G306-P416, brd4(1) N44-E168, brd4(2) K333-E460, brdt(1) N21-E137 and brdt(2) S257-M361 were provided by the Oxford Structural Genomics Consortium (SGC) for expression with an N-terminal His<sub>6</sub>-tag and a TEV protease cleavage site. A plasmid for full-length brd2 protein was purchased from DNASU Plasmid Repository at the Arizona State University and a tandem construct of brd2 containing both bromodomains and the linker region (G73-D455) was cloned into a pCri (11b) vector (based on pET15b, Amp<sup>r</sup>) for expression with an N-terminal His<sub>6</sub>-tag, a Small Ubiquitin-like Modifier (SUMO) tag, and a SUMO protease (SEN1) cleavage site. A pEGFP-C1 plasmid containing the full-length brd4 gene (amino acids 1-1362) for fluorescence recovery after photobleaching experiments (FRAP) was also a gift from the SGC Oxford. Plasmid pcDNA5-FRT/TO-GFP was a gift from Dr Mark Peggie from University of Dundee. Full-length brd4 gene (amino acids 1-1362) was cloned into pcDNA5-FRT/TO-GFP to generate a vector for conditional low-level expression of GFP-tagged brd4 proteins in U2OS cells transfected with pcDNA6/TR in a tetracycline-dependent manner. U2OS cells with transfected pcDNA6/TR were a gift from Dr Eric Griffis (University of Dundee).

A tetra acetylated peptide mimicking the acetylated histone tail H4 (KAc 5, 8, 12, 16), with the sequence YSGRGGK(Ac)GGK(Ac)GLGK(Ac)GGAK(Ac)RHRK (18) was purchased from GenScript.

### Site directed mutagenesis

Single point Leu-to-Ala mutations were introduced using *QuickChange II Site directed Mutagenesis Kit* (Agilent). Primers were designed following the recommendations in the *QuickChange Manual* and oligonucleotides were synthesized, desalted, purified and lyophilized by Sigma Aldrich. The polymerase chain reaction (PCR) was performed on a 2720 Thermal Cycler (Applied Biosystems<sup>®</sup>). Upon digestion of the parental DNA strands by Dpn1 restriction enzyme, the PCR product was transformed into competent *E. coli* DH5 $\alpha$  cells and grown on lysogeny broth (LB) agar plates containing 50  $\mu$ g/mL of kanamycin at 37 °C for 12-16h. Single colonies were then picked from the agar plates and grown for 12h in 10 mL of LB medium containing 50  $\mu$ g/mL of Kanamycin. DNA was subsequently extracted and purified using *QIAprep Spin Miniprep Kit* (Qiagen). Purified DNA was then submitted to sequencing to confirm the presence of the desired mutation.

### Protein expression

Single colonies from freshly transformed plasmid DNA in competent *E. coli* BL21(DE3) cells were grown overnight at 37 °C in 10 mL of LB medium with 50  $\mu$ g/mL kanamycin or ampicillin. The start-up culture was then diluted 1:100 in fresh Terrific-Broth (TB) medium with 50  $\mu$ g/mL of kanamycin or ampicillin and 4 mL of glycerol. Cell growth was allowed at 37 °C and 200 rpm to an optical density of about 2.5 (OD<sub>600</sub>), at which point temperature was decreased to 18°C. Once the cultures equilibrated at 18 °C, the optical density was around 3.0 (OD<sub>600</sub>) and protein expression was induced overnight at 18 °C with 0.1 mM isopropyl- $\beta$ -thiogalactopyranoside (IPTG). The bacteria was harvested the next day by centrifugation (8000 rpm for 10 minutes at 6 °C, JLA 8.1000 rotor on a Beckman Coulter Avanti J-20 XP centrifuge) and frozen at -20 °C as pellets for storage.

### Protein purification

Pellets of cells expressing His<sub>6</sub>-tagged proteins were resuspended in lysis buffer (50 mM HEPES pH 7.5 at 25 °C, 500 mM NaCl, 10 mM Imidazole and 2 mM  $\beta$ -mercaptoethanol). One

tablet of *Complete Protease Inhibitor Cocktail* (Roche) was added to the resuspension and cells were lysed using a French Press at 4 °C. Following a 20 min incubation period at room temperature with 10 µg/mL DNaseI and 10 mM MgCl<sub>2</sub>, the cell debris was removed by centrifugation (20000 rpm for 30 minutes at 6 °C, JA25.50 rotor in a Beckman Coulter Avanti J-20XP centrifuge). The lysate was purified via immobilized metal ion affinity chromatography on a *His Trap HP 5mL* Ni sepharose column (GE Healthcare Life Sciences) on an *ÄKTAexplorer<sup>TM</sup>* system (GE Healthcare) or an *ÄKTApure<sup>TM</sup>* system (GE Healthcare). The column was equilibrated by 25 mL of lysis buffer and the flow was set to 1 mL/min. His<sub>6</sub> tagged protein was eluted using a linear gradient to 250 mM imidazole in the same buffer. For single bromodomain constructs, the His<sub>6</sub> tag was subsequently removed by overnight treatment with Tobacco Etch Virus (TEV) protease at 4 °C followed by a second Ni column to collect the flow through. The same procedure was followed to cleave the SUMO tag from tandem constructs using sentrin-specific protease 1 (SEN1) instead of TEV. After Ni purification, the pooled elution fractions were concentrated to a volume of 4 mL and further purified by size exclusion chromatography on a *Superdex 75 16/60 Hiload* gel filtration column (GE Healthcare) on an *ÄKTAexplorer<sup>TM</sup>* or an *ÄKTApure<sup>TM</sup>* system using the following buffer: 10 mM HEPES pH 7.5 at 25 °C, 500 mM NaCl and 5% glycerol. Samples were monitored by SDS-polyacrylamide gel electrophoresis to verify purity. Pure protein was then flash frozen with liquid nitrogen and stored at -80 °C. The mass and purity of the proteins were subsequently verified by mass spectrometry.

#### Differential scanning fluorimetry

Differential scanning fluorimetry (DSF) assays were performed on a *LightCycler<sup>®</sup> 480* (Roche) or a *Mx3005P Real Time PCR* machine (Stratagene). Prior to DSF assays, frozen proteins were buffer exchanged using Vivaspin<sup>®</sup> 6 concentrators with a 10 kDa cutoff on a *Centrifuge 5430* (Eppendorf) at a speed of 6000xg to remove glycerol and to buffer the proteins in 20 mM HEPES pH 7.5 at 25 °C and 100 mM NaCl. SYPRO<sup>®</sup> Orange (Invitrogen Molecular Probes<sup>®</sup>) was used as a reporter dye to monitor the denaturing process of the proteins. Samples were assayed on a 96-well plate with final protein concentrations of 2 µM for the *LightCycler<sup>®</sup> 480* and 6 µM for *Mx3005P*. Compounds were added at a final concentration of 10 µM for the *LightCycler<sup>®</sup> 480* and 30 µM for *Mx3005P*, while the tetra acetylated histone peptide was added to a final concentration of 100 µM and 300 µM respectively. SYPRO<sup>®</sup> Orange was added at a dilution of 1:1000 and excitation and emission filters for the SYPRO<sup>®</sup> Orange dye were set to 483 nm and 568 nm respectively for the *LightCycler<sup>®</sup> 480* and 465 nm and 590 nm respectively for *Mx3005P*. The temperature was raised with a step of 0.6 °C per minute from 37 °C to 95 °C with the *LightCycler<sup>®</sup> 480* collecting 39 measurements per °C, and 1 °C per minute from 25 °C to 95 °C with *Mx3005P*, collecting fluorescence readings at the end of each interval. Each sample was run in triplicates.

Collected data was analyzed by *IGOR Pro 6* from Wave Metrics, Inc. Analysis was done as recommended by Niesen et al. (19). Fluorescence intensity was plotted as a function of temperature, generating a sigmoidal curve described by a two-state transition from folded to unfolded protein. Curves were fitted by the following sigmoidal equation:

$$f(x) = A_1 + \frac{A_2}{1 + \exp \frac{x_0 - x}{dx}}$$

A<sub>1</sub> and A<sub>2</sub> are the values of minimum and maximum intensities, respectively, x<sub>0</sub> is the inflection point and dx is the rate. Fitted curves were differentiated in *IGOR Pro 6* and the maximum of the first derivative was identified using the same program. These values correspond to the inflection points of the transition curves and thus to the melting temperatures of the proteins (T<sub>m</sub>).

### Bio-layer interferometry

All bio-layer interferometry (BLI) (20) binding experiments were conducted at 25 °C in buffer 10 mM HEPES pH 7.5, 100 mM NaCl on an OctetRed384 instrument (ForteBio). The histone library contained 22 H4 histone peptides with single and multiple acetylation marks (Alta Bioscience Ltd., University of Birmingham). All the peptides contained an aminohexanoic acid spacer and a biotin at their C- terminus to allow immobilization to the streptavidin-coated sensors. The final non-tagged protein concentration of all samples was 20 µM dispensed in a volume of 100 µl per well. Assays were performed in black, 96-well, flat bottom sample plates harbouring gently agitated to 1000 rpm. Common cycles steps for analysis included 120s of biosensor washing step, associations in wells containing the free labelled protein 240s, and dissociations in buffer was allowed to proceed for 240s. Reference subtraction was performed with ForteBio data analysis software to subtract the effect of baseline drift and the effect of nonspecific binding using a buffer control well.

### Isothermal titration calorimetry

Isothermal titration calorimetry (ITC) was carried out on an ITC<sub>200</sub> instrument (MicroCal™, GE Healthcare). Experiments were conducted at three different temperatures 15 °C, 25 °C and 30 °C, while stirring at 1000 rpm. Buffers of proteins, peptide and compounds were matched to 20 mM HEPES pH 7.5 at 25 °C and 100 mM NaCl. Frozen protein was buffer exchanged as described for the DSF experiments. Each titration comprised 1 initial injection of 0.4 µL lasting 0.8s, followed by 19 injections of 2 µL lasting 4s each at 2 min intervals. The initial injection was discarded during data analysis. Standard and reverse titrations were conducted depending on the binding partners.

**Peptide Binding:** Experiments with the tetra acetylated histone peptide were performed at 15 °C. The micro syringe (40 µL) was loaded with a solution of the peptide sample at a concentration of 1-4 mM and it was injected into the cell (200 µL), occupied by a protein at a concentration of 50-100 µM.

**Ligand Binding:** Reverse titrations were conducted to test the binding of I-BET and the bumped ligands **ME** and **ET** to the wild type and L/A mutant single bromodomain proteins. Experiments were carried out either at 25 °C or 30 °C. For strong binders, a concentration of 150-200 µM of the protein was injected into a solution of 15-20 µM compound. For lower affinity interactions, a concentration of 350 µM protein was titrated into a solution of 20 µM compound. In cases where the compound was solubilized in dimethyl sulfoxide, DMSO concentration was adjusted to 1% both in the syringe and in the cell. The titrations of I-BET and **ET** compounds into the tandem proteins (wild type and L/A mutants) were carried at 30°C; the binders at 150 µM concentration were injected into a 15 µM protein solution. Both solutions of compound and protein were adjusted to 1.5% DMSO.

**Data Analysis:** All the data was fitted to a single binding site model using the Microcal LLC ITC200 Origin data analysis software to yield enthalpies of binding ( $\Delta H$ ) and binding constants ( $K_{ds}$ ). Further thermodynamic parameters i.e. changes in entropy  $\Delta S$ , changes in free energy  $\Delta G$  and dissociation constants ( $K_{ds}$ ) were calculated from these values.

### Preparation of human osteosarcoma cells for functional analysis of brd4 mutants

Functional analysis of brd4 experiments were performed in human osteosarcoma U2OS cells transfected with pcDNA6/TR. U2OS were cultured in Opti-MEM supplemented with fetal bovine serum to 70-80% confluency. U2OS cells were transfected with siRNA to suppress the endogenous *brd4*. After 24h, cells were transfected with pcDNA5 constructs containing GFP-tagged brd4 wildtype or mutant constructs using FuGene 6 (Promega) according to manufacturer's instructions. After another 18h, culture medium was changed to fresh medium supplemented with tetracycline to induce expression of GFP-brd4. Cells were harvested by trypsinization 24h after induction. Harvested cells were washed with PBS and were stored at -80 °C.

### Short Interfering RNA (siRNA)

Custom brd4 region-specific siRNA were synthesized from Invitrogen using the following sequences:

3'UTR specific 5'- GGUGAAGAAUGUGAUGGGGAUCACUA-3'

5'UTR specific 5'- AUCAAAGUCAGAAGCCACCUAGGUG-3'

and from Integrated DNA Technologies using the following sequence:

ORF specific 5'- GGAAUGCUCAGGAAUGUAUCCAGGA -3'.

For siRNA experiments, cells were transfected with Lipofectamine RNAiMax (Invitrogen) according to the manufacturer's instructions. MISSION® siRNA Universal Negative Control #1 from Sigma Aldrich was used as negative control.

### Quantitative PCR (qPCR) analysis

Total RNA was extracted with the RNeasy Mini Kit (Qiagen) or GeneJET RNA purification kit (Thermo Scientific) according to the manufacturer's directions. RNA was converted to cDNA using a iScript cDNA synthesis kit (BioRad). For quantitative PCR, PerfeCTa SYBR Green FastMix for iQ kit was used and the samples were prepared according to the manufacturer's protocol and analysed using a Bio-Rad iCycler iQ machine. GAPDH was used as a normalizing gene in all experiments.

Primers used:

Gene	Forward primer (5'→3')	Reverse primer (5'→3')
GAPDH	AACGGGAAGCTTGTCATCAATGGAAA	GCATCAGCAGAGGGGGCAGAG
c-Myc	AATGAAAAGGCCCAAGGTAGTTATCC	GTCGTTTCCGCAACAAGTCTCTTC
p21	AGTCAGTTCCTTGTGGAGCC	GACATGGCGCCTCCTCTG

### Fluorescence recovery after photobleaching

Fluorescence recovery after photobleaching (FRAP) experiments were performed in human osteosarcoma U2OS cells transfected with mammalian expression constructs encoding wild type and mutant GFP chimeras of brd4. Cells were cultured in DMEM (gibco) supplemented with fetal bovine serum, Penicillin/Streptomycin and L-Glutamine. Cells were seeded into glass bottom dishes (WillCo) to about 40% confluency and transfected with the constructs using Effectene (QIAGEN) at least 18h before the experiment. Treatment of cells with 1µM compounds (in DMSO) was performed 12-15h before the experiment. Cells without compound treatment were treated with DMSO as a vehicle control at least 15h before the experiment. DMEM was exchanged for CO<sub>2</sub>-independent phenol red-free media (gibco) for the experiment. FRAP studies were performed using a DeltaVision Core mounted on an Olympus IX70 stand with a 60x 1.4NA plan apo objective lens equipped with a heated chamber set to 37 °C and a Quantifiable Laser Module (QLM) with 10 mW 488 nm solid state laser delivering a diffraction limited spot to the centre field of view. A 490/20 nm excitation and a 528/38 nm emission filter were used. A spot was bleached with a single pulse at 100% laser power for 0.2s and recovery images were acquired using a coolsnap HQ camera with a 2x2 bin at 0.05s exposure. Three pre event images were taken, as well as 32 post event images over the course of 20s in total, the first of which was acquired 0.02s after the bleach event. FRAP data was analysed using the SoftWorX software. It was fitted to a 2-dimensional recovery curve using the method of Axelrod (21) as implemented within the software and half-times of recovery were calculated.

### Docking

A model of the L/A mutant protein was generated by introducing the mutation with the Maestro editing tools, using the crystal structure of brd4(1) (pdb 3P5O (2)) as a template. WT and mutant 3P5O were prepared using the Protein Preparation Wizard (22) from Schrodinger, and the corresponding grids were generated with Glide (23-26). Ligands were prepared (Ligprep (27)) and

docked (Glide) in mutant and WT grids. No constraint was applied to the system. Docking poses were subjected to one round of Prime (28) minimisation, then analysed visually with Maestro and Pymol (29).

### X-ray crystallography

*Crystal structures of unbound brd2(2) L383A mutant.* The purified mutant bromodomain was concentrated to 17 mg/mL, in 20 mM Tris-HCl pH 8, 200 mM NaCl, 2 mM DTT buffer and subjected to sitting-drop vapour diffusion crystal growth screening. Initial crystallization conditions were optimized and scaled-up in hanging drop well plates. The optimized crystallization conditions were 0.1 M Na citrate pH 5.6, 0.2M ammonium sulfate, 30% PEG 4000. Crystals grew at 20 °C and were directly flash-frozen from well solution in liquid nitrogen with 15% glycerol used as the cryo-protectant. Brd2(2) L383A mutant data set was collected *in house* on a X8-Proteum/Bruker AXS system and processed to 1.5 Å with Bruker-Proteum2 and XPREP software. Molecular replacement solutions were determined with the wild type brd2(2) bromodomain (pdb 2DVV) as the searching template using PHASER (30) within the Phenix software suite. The asymmetric unit contained 1 molecule and a solvent content of 47.0%. The initial model was rebuilt with COOT (31), cycled with structure refinement by Refmac5.5 (32) in the CCP4 suite (33). Thermal motions were analyzed using TLSMD (34) and hydrogen atoms were included in late refinement cycles. The final model was deposited to the protein data bank under accession number 4QEU.

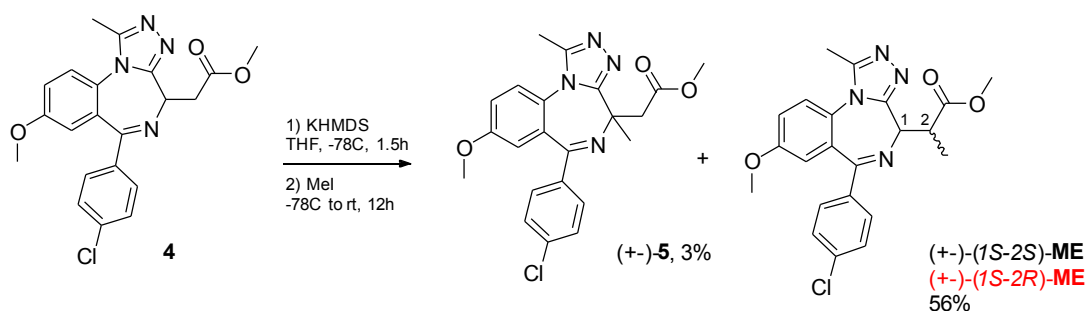
*Crystal structure of brd2(2) L383A mutant in complex with ME and ET.* The protein was concentrated up to 17 mg/mL in 20 mM Tris-HCl pH 8, 200 mM NaCl, 2 mM DTT buffer and co-crystallized with 2:1 excess of compound ME and ET separately. Crystals were grown in hanging drop diffusion plates in 1 µL + 1 µL drop ratio under the crystallization condition 0.1 M Hepes pH 7, 0.2 M Imidazole, 41% PEG 400. Crystals were cryo-protected, flash-frozen and X-ray diffraction data were collected at 100 K at a X8-Proteum/Bruker AXS home source. Datasets were processed to 1.8 Å for the complex with ME, and 1.7 Å for the complex with ET using XDS and SCALA. Structures were solved by molecular replacement using PHASER (pdb 2DVV was used as the searching template) and were refined through iterative rounds of building/refinement in COOT (31) and Refmac5.5 (32). Their respective ASU contained one molecule and 45.6 and 45.0 % of solvent content. The final models were deposited to the protein data bank under accession code 4QEV and 4QEW respectively. The crystallographic statistics for all dataset collections and refined coordinates are given in Table S4.

### General synthetic procedures

All reagents and solvents were obtained from commercial sources, and used as supplied unless otherwise indicated. Reactions requiring anhydrous conditions were conducted in heated glassware (heat gun), under an inert atmosphere (argon), and using anhydrous solvents. CH<sub>2</sub>Cl<sub>2</sub> and MeOH were distilled over CaH<sub>2</sub>. THF and Et<sub>2</sub>O were distilled on Na/benzophenone. Toluene was distilled over Na. All reactions were monitored by analytical thin-layer chromatography (TLC) using indicated solvent systems on E. Merck silica gel 60 F254 plates (0.25 mm). TLC plates were visualized using UV light (254 nm) and/or by staining in potassium permanganate followed by heating. Solvents were removed by rotary evaporator below 40°C and the compounds further dried using high vacuum pumps.

<sup>1</sup>H and <sup>13</sup>C NMR were recorded on a Bruker Advance 400 spectrophotometer at 400 MHz and 100 MHz respectively. Chemical shifts (δ H) are quoted in ppm (parts per million) and referenced to residual solvent signals: <sup>1</sup>H δ = 7.26 (CDCl<sub>3</sub>), 2.50 (*d*<sub>6</sub>-DMSO), 3.31 (CD<sub>3</sub>OD), <sup>13</sup>C δ = 77.0 (CDCl<sub>3</sub>), 39.43 (*d*<sub>6</sub>-DMSO), 49.05 (CD<sub>3</sub>OD). Coupling constants (*J*) are given in Hz. High resolution mass spectra (ESI) were recorded on a Waters LCT Premier Mass Spectrometer.

## 1) Synthesis of ME



Methylation of the ternary centre and the side chain:

Compound **4** was synthesized as previously described (2). A -78 °C solution of **4** (400 mg, 0.973 mmol, 1.0 eq.) in freshly distilled THF (6 mL), under Ar, was added dropwise by cannulation to a -78 °C solution of KHMDS (0.5 M in toluene, 2.34 mL, 1.17 mmol, 1.2 eq.) in freshly distilled THF (14 mL), under Ar. The resulting dark solution was stirred at -78 °C for 1h. MeI (73 µL, 1.17 mmol, 1.2 eq.) was then added dropwise, and stirring was continued for 1h at -78 °C. The temperature of the acetone bath was then gradually increased to rt over a few hours, and the mixture was stirred overnight at rt. The reaction was quenched with a few drops of AcOH and concentrated to dryness. The residue was partitioned between saturated aqueous NaHCO<sub>3</sub> and CHCl<sub>3</sub> and the aqueous phase was extracted 3 times with CHCl<sub>3</sub>. The combined organic layers were dried (MgSO<sub>4</sub>) and concentrated. NMR of the crude material revealed the formation of a mixture of (+)-**5**, (+)-(1S-2S)-**ME**, (+)-(1S-2R)-**ME** and (+)-**4**. Purification by flash column chromatography (PE<sub>40-60</sub>/acetone 6:4) afforded a mixture of (+)-(1S-2S)-**ME** and (+)-(1S-2R)-**ME** (232 mg, 56%) and (+)-**5** (14 mg, 3%).

### (+)-methyl (S)-2-((S)-6-(4-chlorophenyl)-8-methoxy-1-methyl-4H-benzo[f][1,2,4]triazolo[4,3-a][1,4]diazepin-4-yl)propanoate ((+)-(1S-2S)-**ME**)

(+)-(1S-2S)-**ME** was the major product of the alkylation reaction and migrated faster than (+)-(1S-2R)-**ME** on silica (PE<sub>40-60</sub>/acetone).

Diastereomerically pure samples of (+)-(1S-2S)-**ME** were obtained after purification by flash column chromatography of the mixture described above. R<sub>f</sub> 0.15 (PE<sub>40-60</sub>/acetone 6:4); <sup>1</sup>H NMR (400 MHz, CDCl<sub>3</sub>) δ 1.60 (d, *J* = 7.2 Hz, 3H), 2.61 (s, 3H), 3.72 (s, 3H), 3.80-3.93 (m, 4H), 4.29 (d, *J* = 10 Hz, 1H), 6.90 (d, *J* = 2.9 Hz, 1H), 7.21 (dd, *J* = 8.8, 2.9 Hz, 1H), 7.34 (m, 2H), 7.41 (d, *J* = 8.8 Hz, 1H), 7.53 (m, 2H); <sup>13</sup>C NMR (100 MHz, CDCl<sub>3</sub>) δ 12.1, 15.4, 41.0, 52.0, 55.9, 57.7, 115.9, 117.7, 125.0, 126.5, 128.5, 130.0, 130.7, 137.0, 137.1, 150.2, 156.0, 158.0, 166.2, 175.9; HRMS (ESI+) *m/z* calc. for C<sub>22</sub>H<sub>22</sub>ClN<sub>4</sub>O<sub>3</sub> [M+H]<sup>+</sup> 425.1375, found: 425.1951.

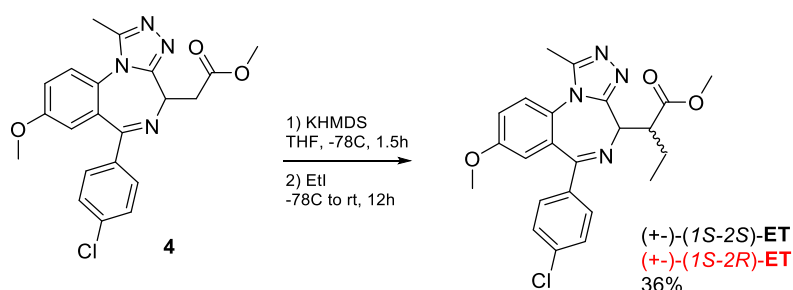
### (+)-methyl (R)-2-((S)-6-(4-chlorophenyl)-8-methoxy-1-methyl-4H-benzo[f][1,2,4]triazolo[4,3-a][1,4]diazepin-4-yl)propanoate ((+)-(1S-2R)-**ME**)

(+)-(1S-2R)-**ME** was the minor product of the alkylation reaction and migrated slower than (+)-(1S-2S)-**ME** on silica (PE<sub>40-60</sub>/acetone).

\*\*\*(+)-(1S-2R)-**ME** is simply referred as **ME** in the manuscript.\*\*\*

To a diastereomeric mixture of (+-)-(1S-2S)-**ME** and (+-)-(1S-2R)-**ME** (50 mg, 0.118 mol, 1 eq.) in anhydrous MeOH (15 mL) was added MeONa (64 mg, 1.18 mmol, 10 eq.). The resulting solution was heated at 120 °C for 40 minutes under microwave irradiation. The reaction mixture was cooled to 60 °C and a few drops of AcOH were added to quench MeONa, followed by cooling to rt and concentration *in vacuo*. The residue was dissolved in sat. aq. NaHCO<sub>3</sub> and extracted 4 times with CHCl<sub>3</sub>. The combined organic layers were dried (MgSO<sub>4</sub>) and concentrated *in vacuo*. Purification by preparative TLC (PE<sub>40-60</sub>/acetone 1:1) afforded diastereomerically pure samples of (+-)-(1S-2R)-**ME**. R<sub>f</sub> 0.15 (PE<sub>40-60</sub>/acetone 6:4); <sup>1</sup>H NMR (400 MHz, CDCl<sub>3</sub>) δ 1.49 (d, *J* = 7.0 Hz, 3H), 2.65 (s, 3H), 3.81 (s, 3H), 3.82 (s, 3H), 4.04 (m, 1H), 4.26 (d, *J* = 10.7 Hz, 1H), 6.89 (d, *J* = 2.8 Hz, 1H), 7.23 (dd, *J* = 8.9, 2.8 Hz, 1H), 7.32 (m, 2H), 7.40-7.48 (m, 3H). <sup>13</sup>C NMR (100 MHz, CDCl<sub>3</sub>) δ 12.0, 15.2, 42.3, 51.9, 55.9, 59.5, 115.9, 117.9, 125.0, 126.0, 128.5, 130.0, 130.8, 136.8, 137.0, 150.5, 155.0, 158.2, 165.5, 175.9; HRMS (ESI+) *m/z* calc. for C<sub>22</sub>H<sub>22</sub>ClN<sub>4</sub>O<sub>3</sub> [M+H]<sup>+</sup> 425.1375, found: 425.1902.

## 2) Synthesis of ET



Ethylation of the side chain:

A -78 °C solution of **4** (400 mg, 0.973 mmol, 1.0 eq.) in freshly distilled THF (6 mL), under Ar, was added dropwise by canulation to a -78 °C solution of KHMDS (0.5M in toluene, 2.34 mL, 1.17 mmol, 1.2 eq.) in freshly distilled THF (14 mL), under Ar. The resulting dark solution was stirred at -78 °C for 1h. Ethyl iodide (94 μL, 1.17 mmol, 1.2 eq.) was then added dropwise, and stirring was continued for 1h at -78 °C. The temperature of the acetone bath was then gradually increased to rt over a few hours, and the mixture was stirred overnight at rt. The reaction was quenched with a few drops of AcOH and concentrated to dryness. The residue was partitioned between saturated aqueous NaHCO<sub>3</sub> and CHCl<sub>3</sub> and the aqueous phase was extracted 3 times with CHCl<sub>3</sub>. The combined organic layers were dried (MgSO<sub>4</sub>) and concentrated. NMR of the crude material revealed the formation of a mixture of (+-)-(1S-2S)-**ET**, (+-)-(1S-2R)-**ET** and (+-)-**4**. Purification by flash column chromatography (PE<sub>40-60</sub>/acetone 6:4) afforded a mixture of (+-)-(1S-2S)-**ET** and (+-)-(1S-2R)-**ET** (152 mg, 36%).

**(+)-methyl (R)-2-((S)-6-(4-chlorophenyl)-8-methoxy-1-methyl-4H-benzo[f][1,2,4]triazolo[4,3-a][1,4]diazepin-4-yl)butanoate ((+)-(1S-2R)-ET)**

(+)-(1S-2R)-**ET** was the minor product of the alkylation reaction and migrated faster than (+)-**14** on silica (CH<sub>2</sub>Cl<sub>2</sub>/MeOH).

\*\*\*(+)-(1S-2R)-**ET** is simply referred as **ET** in the manuscript.\*\*\*

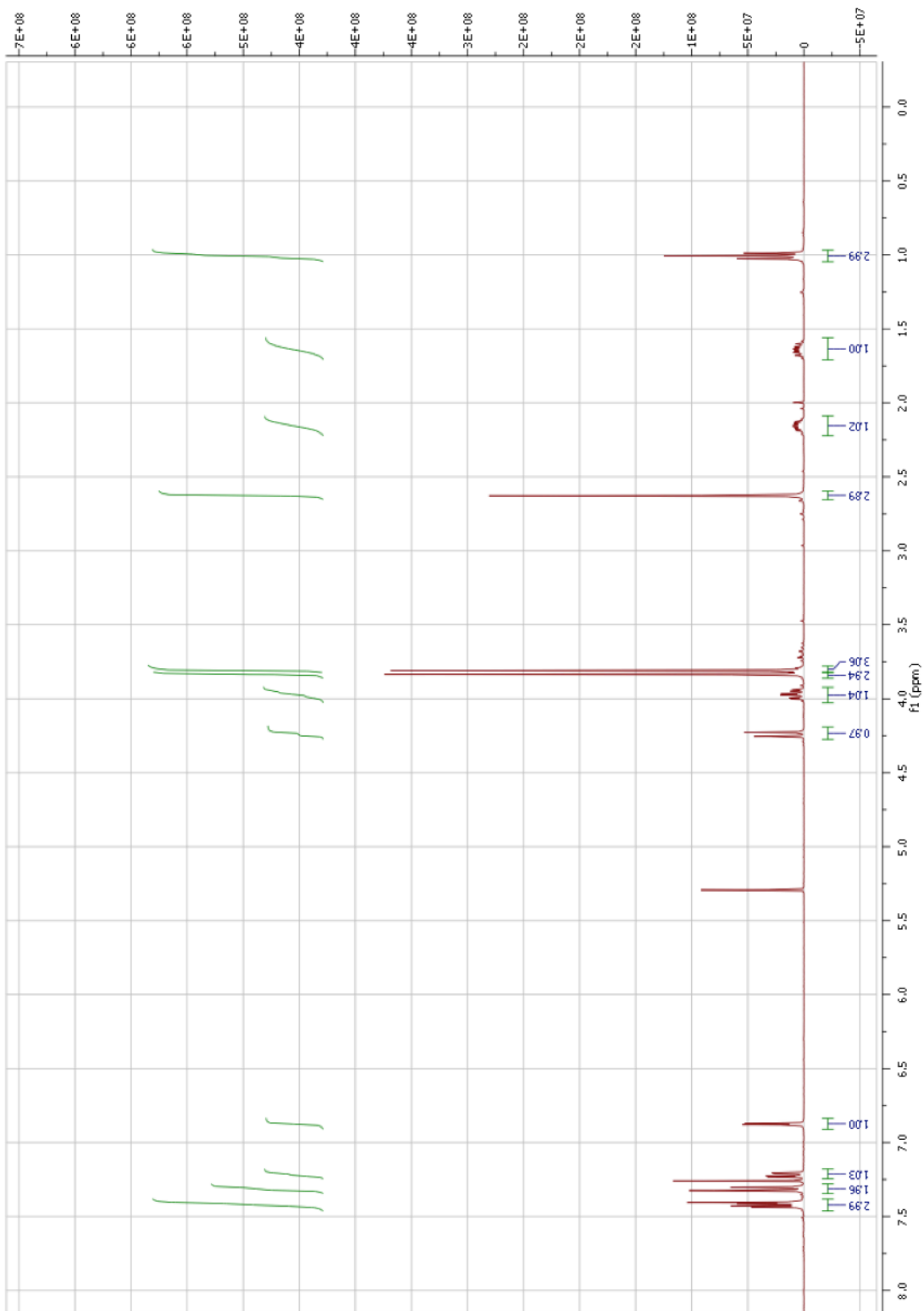


To a diastereomeric mixture of (+-)-(1S-2S)-**ET** and (+-)-(1S-2R)-**ET** (50 mg, 0.114 mol, 1 eq.) in anhydrous MeOH (15 mL) was added MeONa (62 mg, 1.14 mmol, 10 eq.). The resulting solution was heated at 120 °C for 40 minutes under microwave irradiation. The reaction mixture was cooled to 60 °C and a few drops of AcOH were added to quench MeONa, followed by cooling to rt and concentration *in vacuo*. The residue was dissolved in sat. aq. NaHCO<sub>3</sub> and extracted 4 times with CHCl<sub>3</sub>. The combined organic layers were dried (MgSO<sub>4</sub>) and concentrated *in vacuo*. Purification by flash column chromatography (gradient CH<sub>2</sub>Cl<sub>2</sub>/MeOH 98:2 to 96:4) afforded diastereomerically pure samples of (+-)-(1S-2R)-**ET**. R<sub>f</sub> 0.15 (PE<sub>40-60</sub>/acetone 6:4); <sup>1</sup>H NMR (400 MHz, CDCl<sub>3</sub>) δ 1.01 (t, *J* = 7.4 Hz, 3H), 1.64 (m, 1H), 2.16 (m, 1H), 2.63 (s, 3H), 3.81 (s, 3H), 3.84 (s, 3H), 3.97 (m, 1H), 4.24 (d, *J* = 11.0 Hz, 1H), 6.88 (d, *J* = 2.8 Hz, 1H), 7.22 (dd, *J* = 9.0, 2.9 Hz, 1H), 7.31 (m, 2H), 7.39-7.46 (m, 3H); <sup>13</sup>C NMR (100 MHz, CDCl<sub>3</sub>) δ 11.6, 11.9, 23.1, 49.5, 51.6, 55.9, 58.6, 115.9, 118.0, 125.1, 125.7, 128.5, 130.0, 130.7, 136.7, 137.1, 150.5, 155.0, 158.4, 165.6, 175.3; HRMS (ESI+) *m/z* calc. for C<sub>23</sub>H<sub>24</sub>ClN<sub>4</sub>O<sub>3</sub> [M+H]<sup>+</sup> 439.1531, found: 439.2110.

**(+)-methyl (S)-2-((S)-6-(4-chlorophenyl)-8-methoxy-1-methyl-4H-benzo[f][1,2,4]triazolo[4,3-a][1,4]diazepin-4-yl)butanoate ((+)-(1S-2S)-**ET**)**

(+)-(1S-2S)-**ET** was the major product of the alkylation reaction and migrated slower than (+)-(1S-2R)-**ET** on silica (CH<sub>2</sub>Cl<sub>2</sub>/MeOH).

Purification by flash column chromatography (gradient CH<sub>2</sub>Cl<sub>2</sub>/MeOH 98:2 to 96:4) afforded diastereomerically pure samples of (+-)-(1S-2S)-**ET**. R<sub>f</sub> 0.15 (PE<sub>40-60</sub>/acetone 6:4); <sup>1</sup>H NMR (400 MHz, CDCl<sub>3</sub>) δ 1.03 (t, *J* = 7.4 Hz, 3H), 1.84 (m, 1H), 2.30 (m, 1H), 2.59 (s, 3H), 3.72 (s, 3H), 3.78-3.86 (m, 4H), 4.29 (d, *J* = 11.0 Hz, 1H), 6.88 (d, *J* = 2.8 Hz, 1H), 7.21 (dd, *J* = 9.0, 2.8 Hz, 1H), 7.34 (m, 2H), 7.41 (d, *J* = 9.0 Hz, 1H), 7.51 (m, 2H); <sup>13</sup>C NMR (100 MHz, CDCl<sub>3</sub>) δ 11.0, 12.0, 23.1, 47.3, 51.9, 56.0, 56.5, 116.1, 117.7, 125.1, 125.6, 128.6, 130.1, 130.7, 136.8, 137.2, 150.4, 155.9, 158.5, 166.3, 175.0; HRMS (ESI+) *m/z* calc. for C<sub>23</sub>H<sub>24</sub>ClN<sub>4</sub>O<sub>3</sub> [M+H]<sup>+</sup> 439.1531, found: 439.2122.



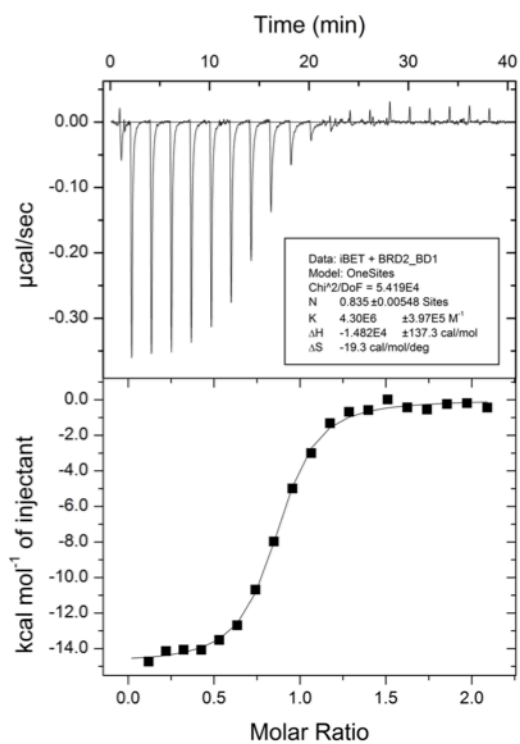
$^1\text{H}$  NMR spectrum of ET

## Supplementary Text

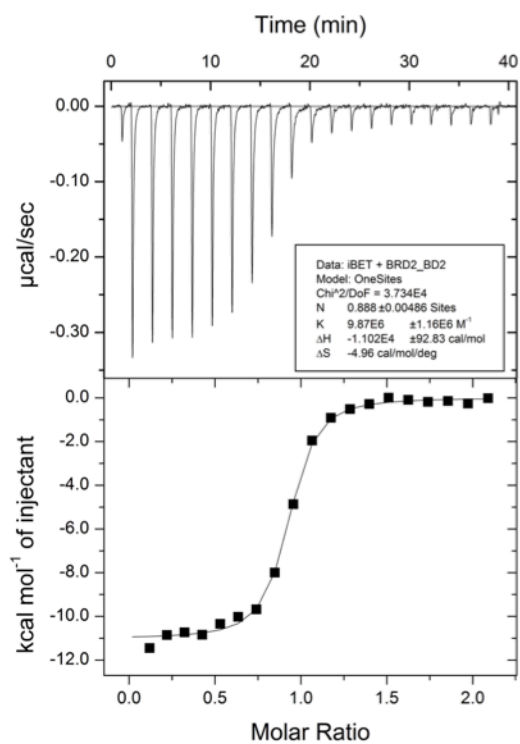
### References and Notes:

18. M. Philpott *et al.*, Bromodomain-peptide displacement assays for interactome mapping and inhibitor discovery. *Mol. Biosyst.* **7**, 2899-2908 (2011).
19. F. H. Niesen, H. Berglund, M. Vedadi, The use of differential scanning fluorimetry to detect ligand interactions that promote protein stability. *Nat Protoc.* **2**, 2212-2221 (2007).
20. E. Martin *et al.* In: M. Cooper and L. M. Mayr (Eds.) Label-free technologies for drug discovery. Wiley (2011).
21. D. Axelrod, D.E. Koppel, J. Schlessinger, E. Elson, W.W. Webb, Mobility measurement by analysis of fluorescence photobleaching recovery kinetics. *Biophys. J.* **16**, 1055-1069 (1976).
22. Schrodinger Suite 2011; Epik version 2.2, LLC, New York, NY, 2011; Impact version 5.7, Schrodinger, LLC, New York, NY, 2011; Prime version 2.3, Schrodinger, LLC, New York, NY, 2011.
23. Glide, version 5.8, Schrodinger, LLC, New York, NY, 2011.
24. R. A. Friesner *et al.*, Glide: A new approach for rapid, accurate docking and scoring. 1. Method and Assessment of docking accuracy. *J. Med. Chem.* **47**, 1739-1749 (2004).
25. T. A. Halgren *et al.*, Glide: a new approach for rapid, accurate docking and scoring. 2. Enrichment factors in database screening. *J. Med. Chem.* **47**, 1750-1759 (2004).
26. R. A. Friesner *et al.*, Extra precision Glide: docking and scoring incorporating model of hydrophobic enclosure for protein-ligand complexes. *J. Med. Chem.* **49**, 6177-6196 (2006).
27. LigPrep version 2.5, LLC, New York, NY, 2011.
28. Prime version 3.0, LLC, New York, NY, 2011.
29. The PyMOL Molecular Graphics System version 1.5.0.4, LLC.
30. A. J. McCoy, Solving structures of protein complexes by molecular replacement with Phaser. *Acta Cryst.* **D63**, 32-41 (2007).
31. P. Emsley, K. Cowtan, Coot: model-building tools for molecular graphics. *Acta Cryst.* **D60**, 2126-2132 (2004).
32. G. N. Murshudov *et al.*, REFMAC5 for the refinement of macromolecular crystal structures. *Acta Cryst.* **D67**, 355-367 (2011).
33. S. Bailey, The CCP4 suite - Programs for protein crystallography. *Acta Cryst.* **D50**, 760-763 (1994).
34. J. Painter, E. A. Merritt, Optimal description of a protein structure in terms of multiple groups undergoing TLS motion. *Acta Cryst.* **D62**, 439-450 (2006).
35. M. M. Matzuk *et al.*, Small-molecule inhibition of BRDT for male contraception. *Cell* **150**, 673-684 (2012).
36. Floyd, S. R. *et al.* The bromodomain protein Brd4 insulates chromatin from DNA damage signalling. *Nature* **498**, 246-250 (2013).

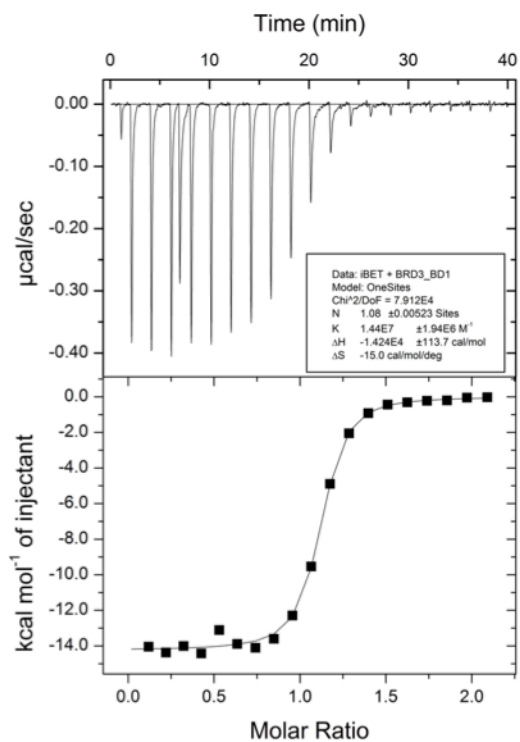
A)



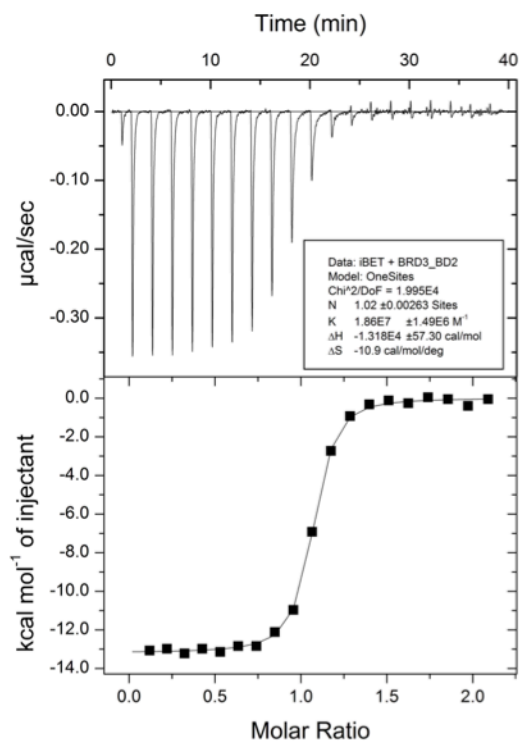
B)



C)



D)



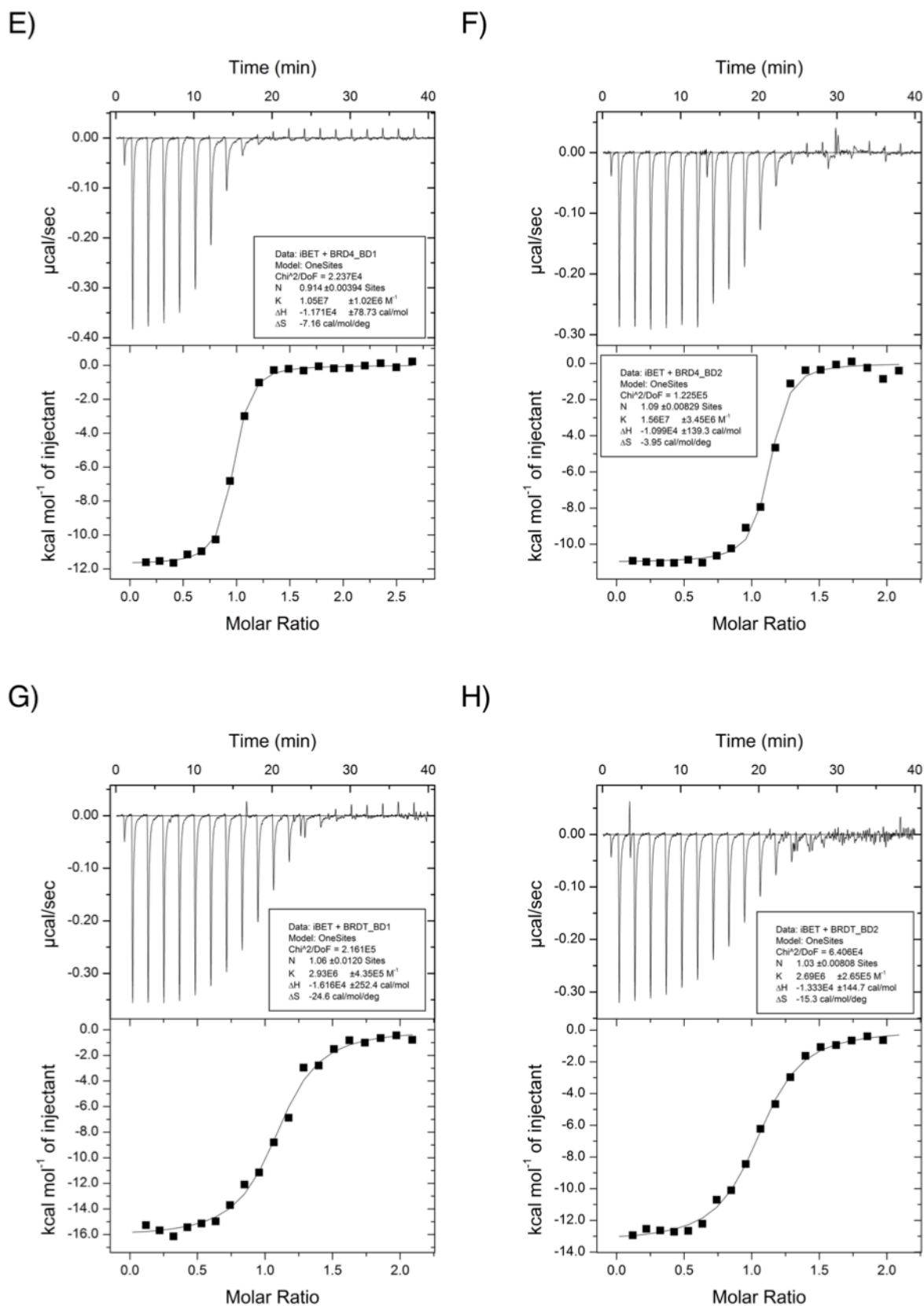
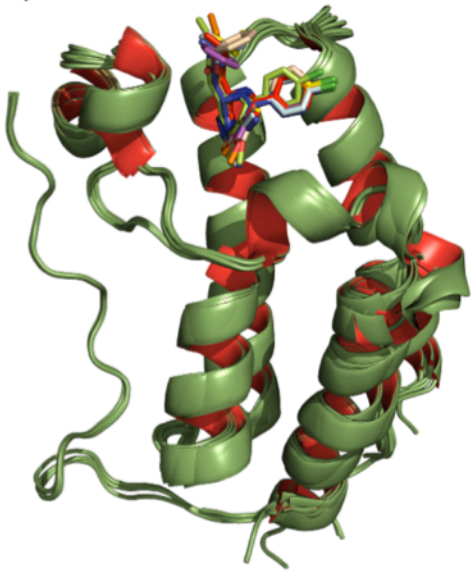


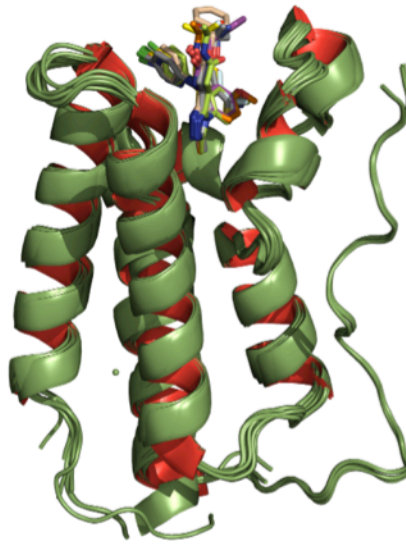
**Fig. S1.**

ITC titration curves for the binding of WT BET bromodomains to I-BET. A) brd2(1); B) brd2(2); C) brd3(1); D) brd3(2); E) brd4(1); F) brd4(2); G) brdt(1); H) brdt(2). Conditions: reverse titrations of WT BET bromodomains (150 µM) into I-BET (15 µM) at 25 °C.

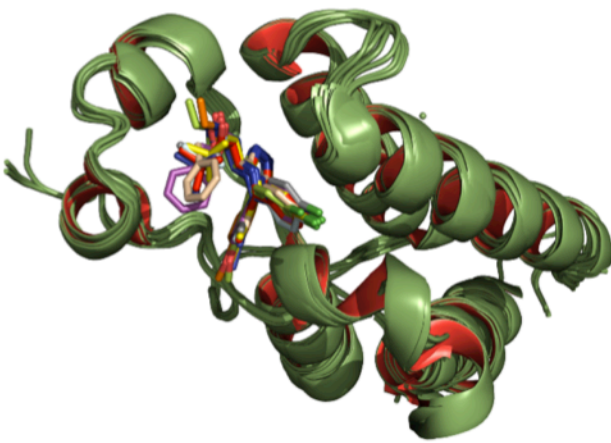
A)



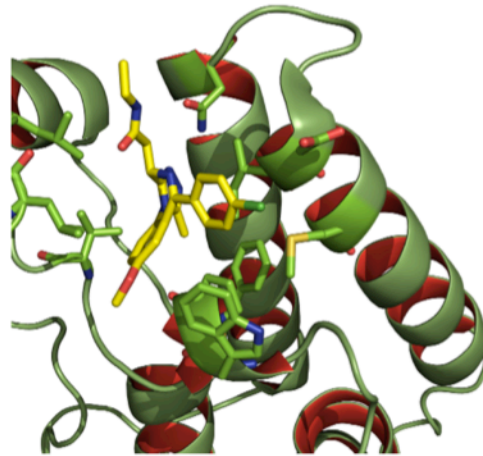
B)



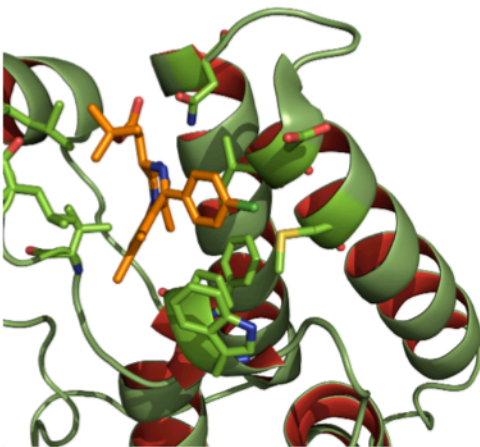
C)



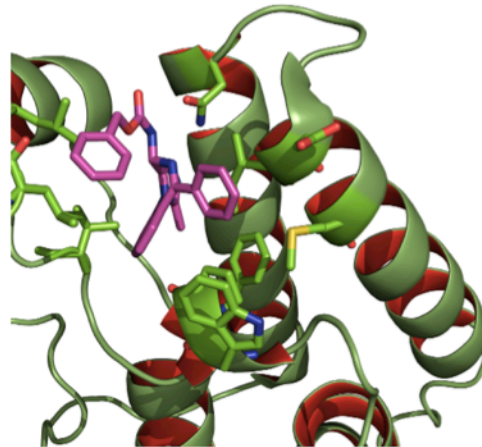
D)



E)

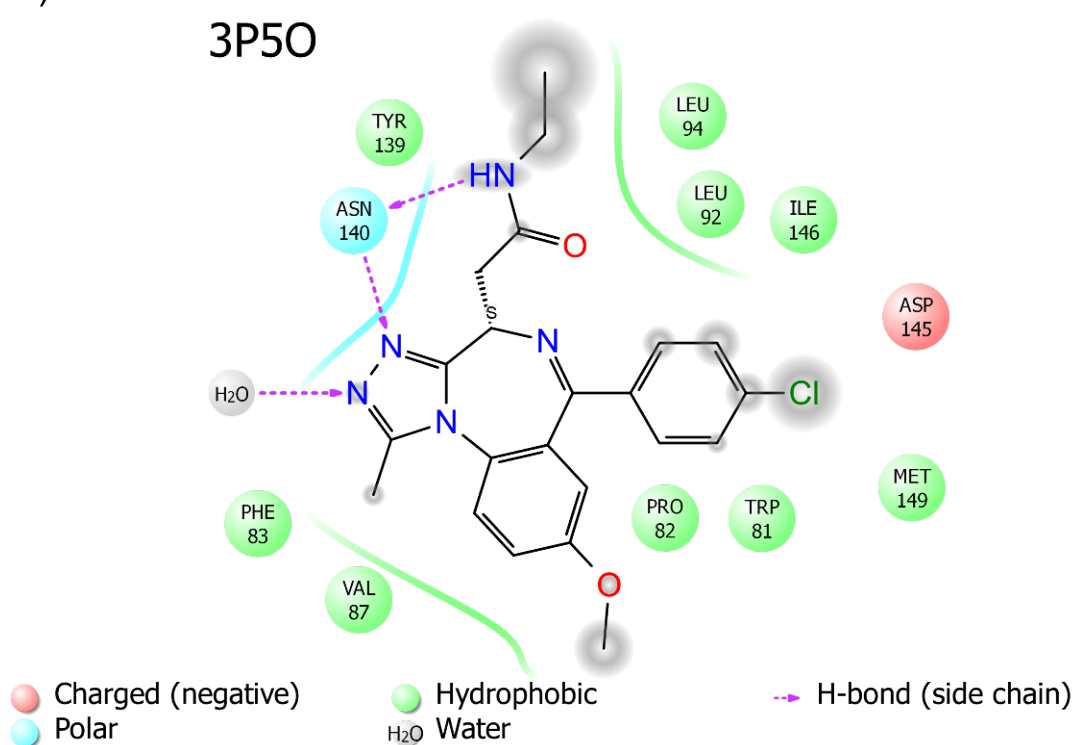


F)



G)

3P5O

**Fig. S2.**

Structural analyses of triazolodiazepine inhibitors bound to BET bromodomains. A) Superposition of 9 structures of BET bromodomains (2-4, 35) in complex with I-BET (1), JQ1 (2) or GW841819X (3) reveals the high degree of structural conservation in the binding site, in addition to the highly conserved binding mode of these ligands. B) Backview; C) Top view; D) I-BET (yellow carbons, stick representation) bound to brd4(1) (green carbons, ribbon and stick representation, pdb 3P5O); E) JQ1 (orange carbons, stick representation) bound to brd4(1) (green carbons, ribbon and stick representation, pdb 3MXF); F) GW841819X (purple carbons, stick representation) bound to brd4(1) (green carbons, ribbon and stick representation, pdb 2YEL); G) Interaction diagram of I-BET with brd4(1) (pdb 3P5O).

PDB code	protein	ligand	resolution	reference
2YEK	brd2(1)	I-BET	1.98	(4)
3ONI	brd2(2)	JQ1	1.61	(3)
3S91	brd3(1)	JQ1	2.06	(unpublished)
3S92	brd3(2)	JQ1	1.36	(unpublished)
2YEL	brd4(1)	GW841819X	1.65	(4)
3MXF	brd4(1)	JQ1	1.60	(3)
3P5O	brd4(1)	I-BET	1.60	(2)
2YEM	brd4(2)	GW841819X	2.30	(4)
4FLP	brdt(1)	JQ1	2.23	(35)





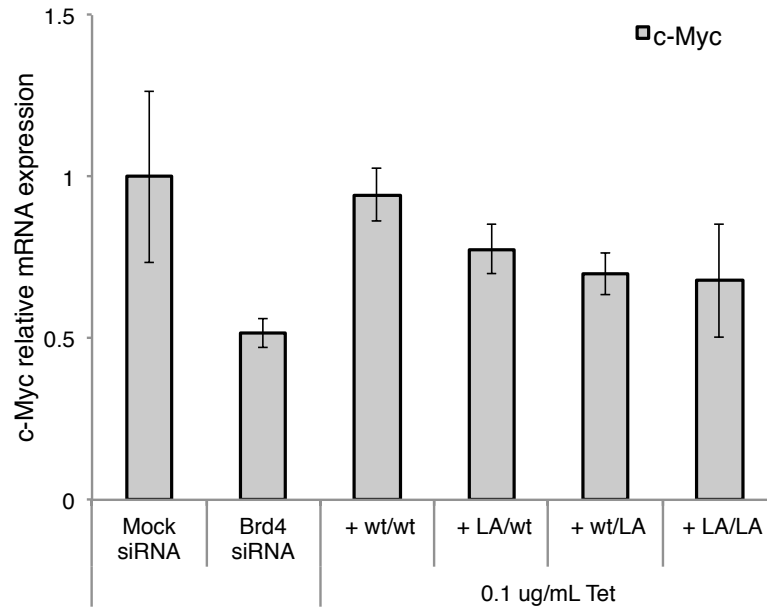


**Fig. S4.**

Function of endogenous brd4 can be restored by exogenous brd4 WT and mutants. U2OS cells were transfected with siRNA suppressing endogenous brd4. c-Myc mRNA level was monitored by qPCR. Reduction of c-Myc mRNA was observed upon siRNA suppression of brd4, as previously reported (36). Four GFP-brd4 constructs (WT, the two singly-mutated L/A, and the doubly-mutated L/A in both bromodomains) were expressed individually at 0.1  $\mu$ g/mL tetracycline induction in cells with suppressed endogenous brd4. Rescue of c-Myc mRNA levels show that the mutants are competent to brd4 function. The data shown represent the mean  $\pm$  standard deviations of three measurements.

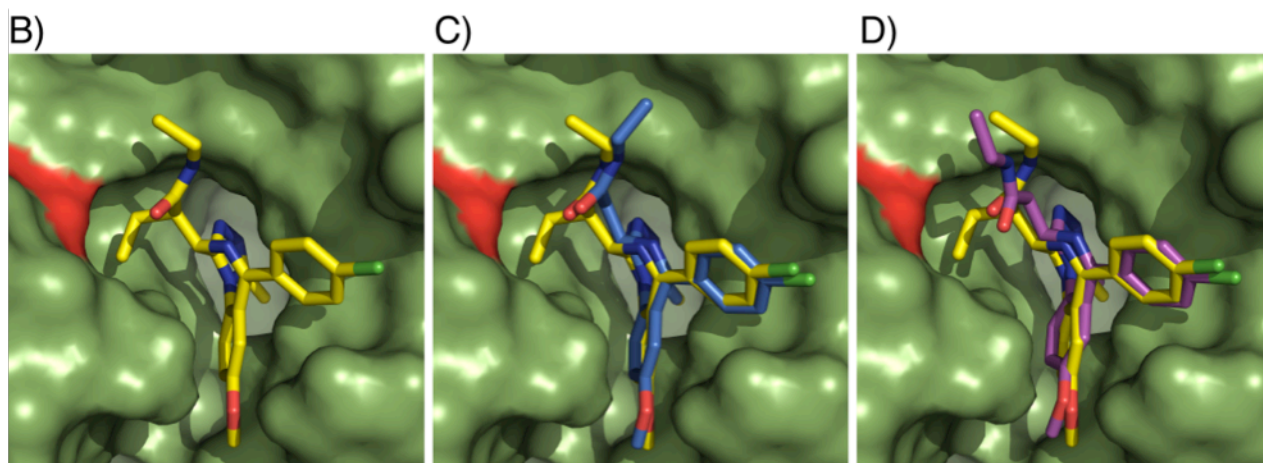
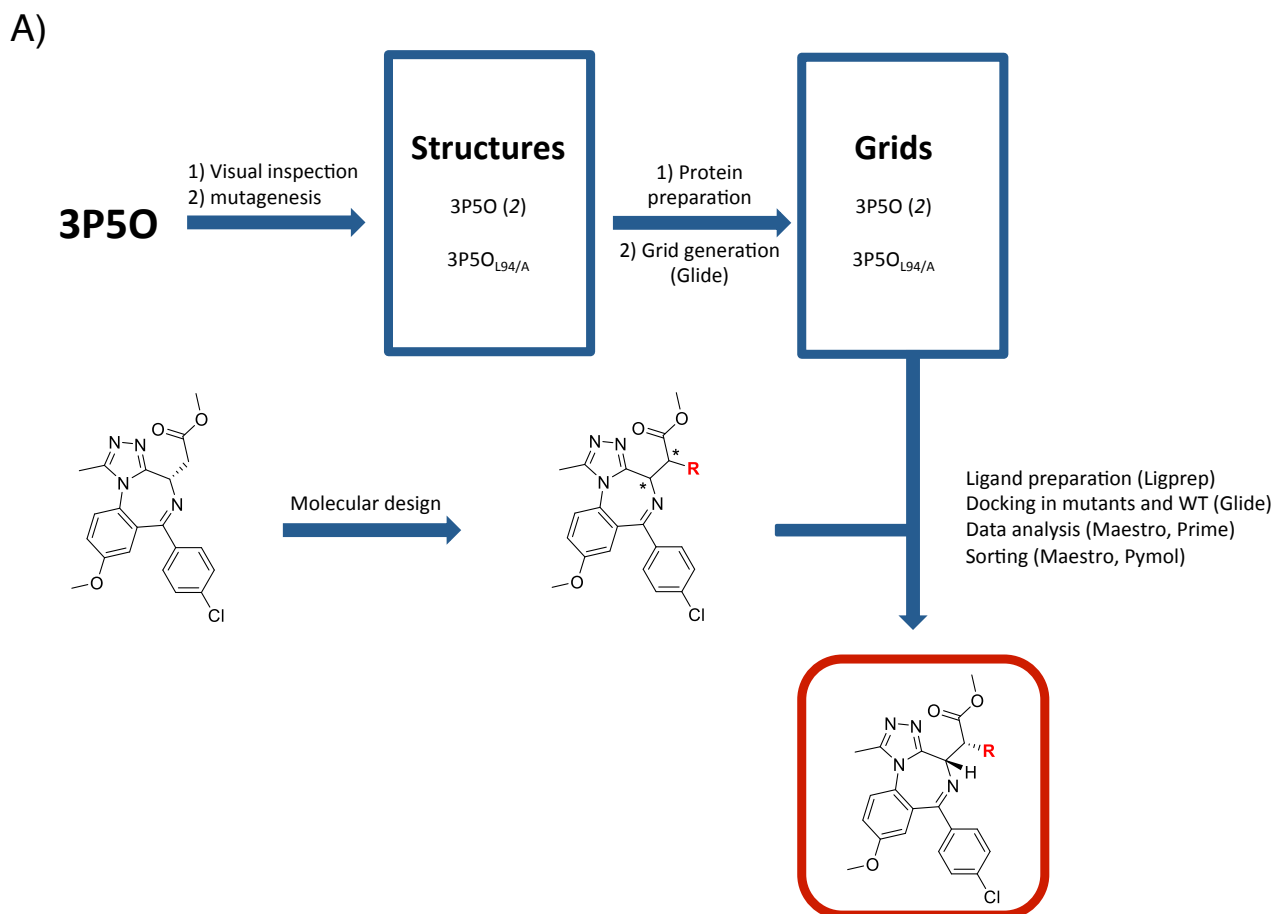


**Fig. S5.**

Docking studies of bumped ligands. A) Workflow. B) An ethyl functionalized I-BET analogue (shown as sticks with yellow carbons) docked into a model L/A mutant derived from 3P5O (green, surface representation). C) An ethyl functionalized I-BET analogue (yellow carbons) docked in the model L/A mutant superimposed with I-BET (blue carbons) docked in 3P5O. D) An ethyl functionalized I-BET analogue (yellow carbons) docked in the model L/A mutant superimposed with the crystal structure 3P5O (I-BET ligand shown with purple carbons). In each case, the alanine residue at the mutation site is shown in red.

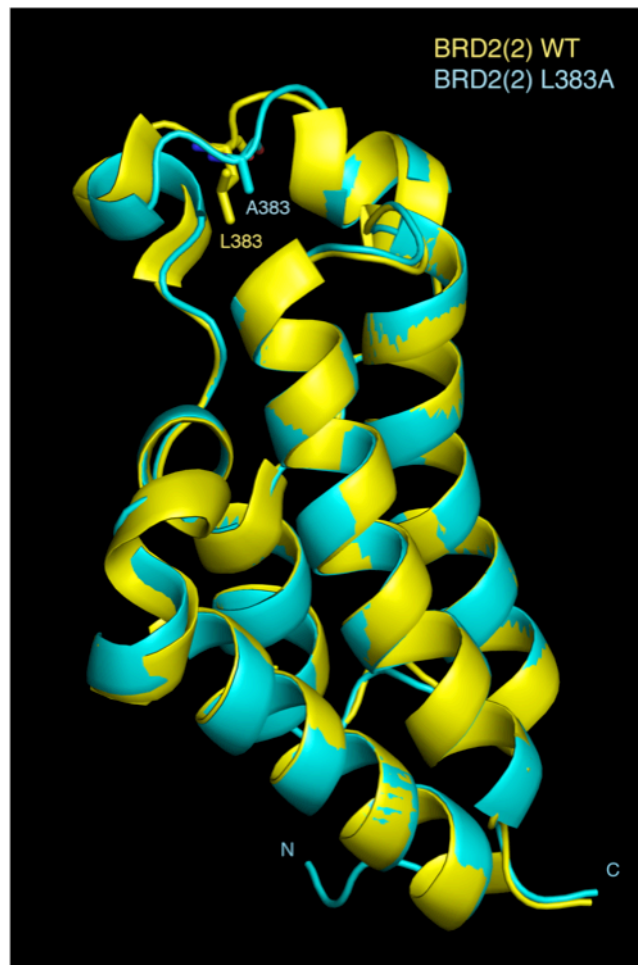
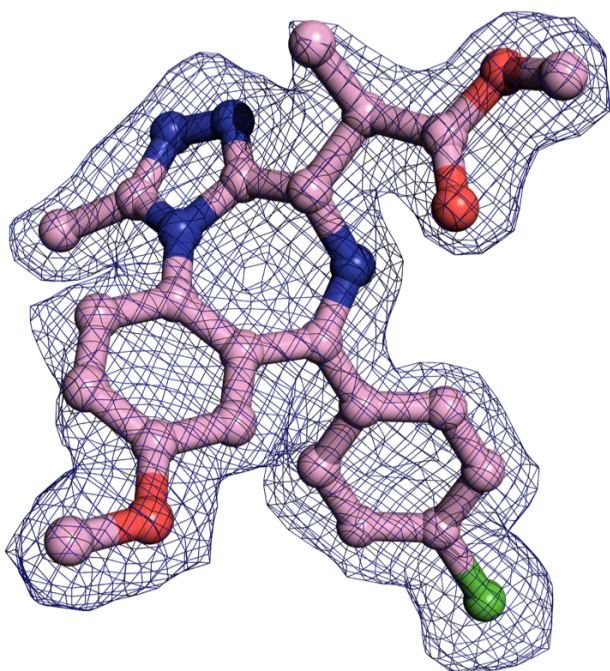


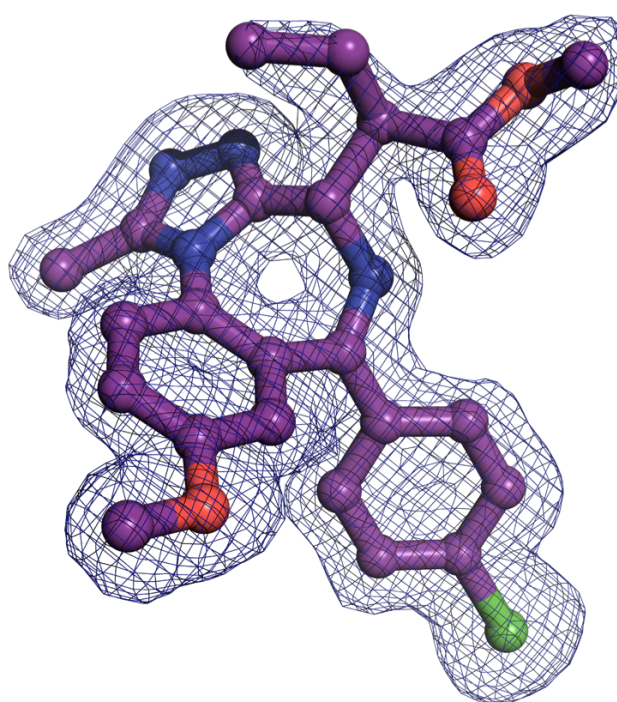
**Fig. S6.**

An L/A mutant retain the same overall fold as WT protein. Crystal structures of brd2(2) L383A in the apo form (pdb 4QEU, cyan) is shown superposed over the crystal structure of the respective WT protein (pdb 3ONI (3), yellow) in complex with JQ1 (inhibitor not shown for clarity). Protein backbones are shown as ribbon representation, with the Leu and Ala residues at position 383 shown in stick. RMSD of main chain atoms = 0.22 Å.

A)



B)

**Fig. S7.**

$|2F_o| - |F_c|$  electron density map contoured at  $1\sigma$  around bound (A) **ME** and (B) **ET** ligands. The ligands are shown as sticks representation with pink (**ME**) and purple (**ET**) carbons, nitrogen atoms in blue, oxygen atoms in red and chlorine atom in green.

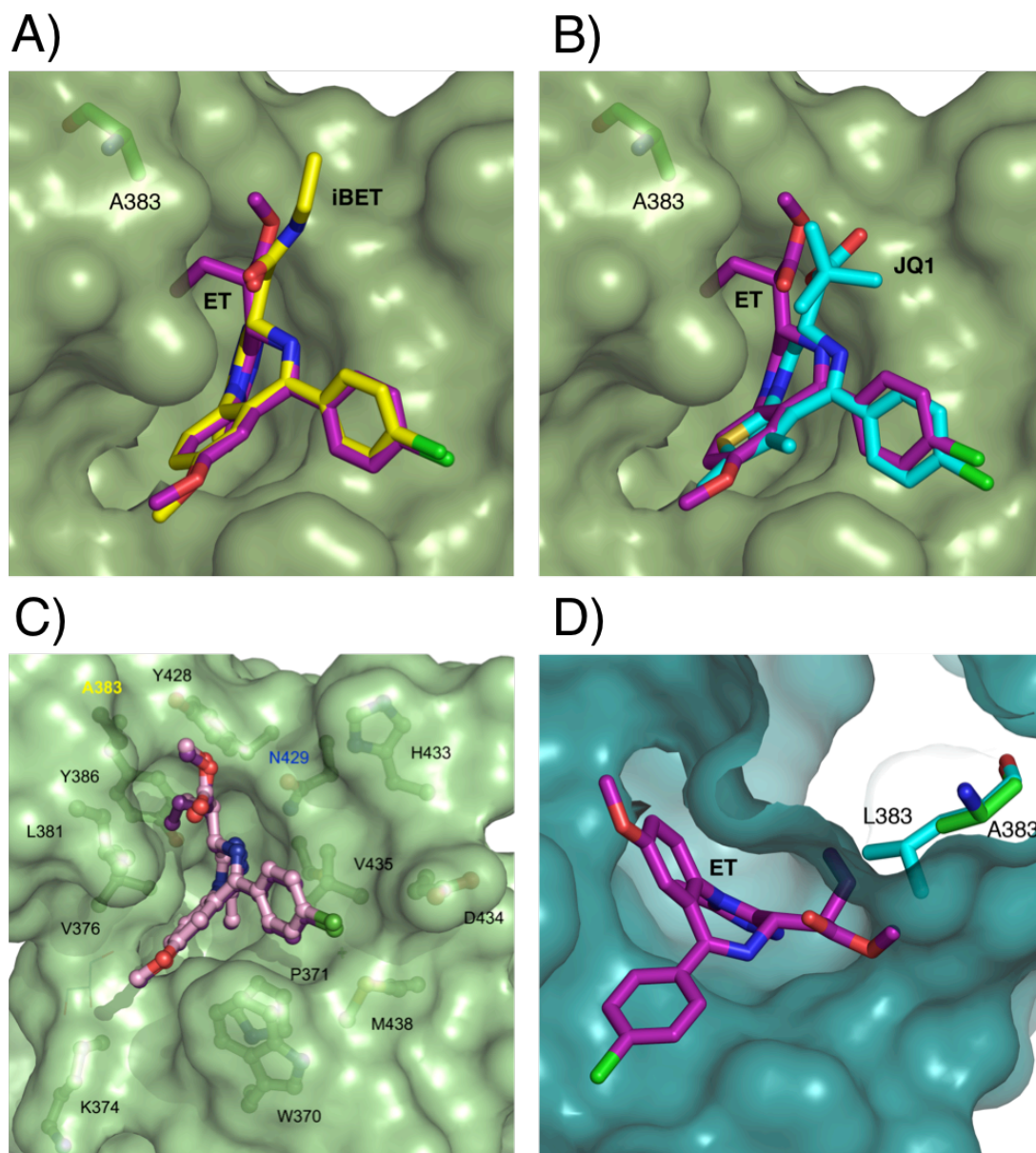
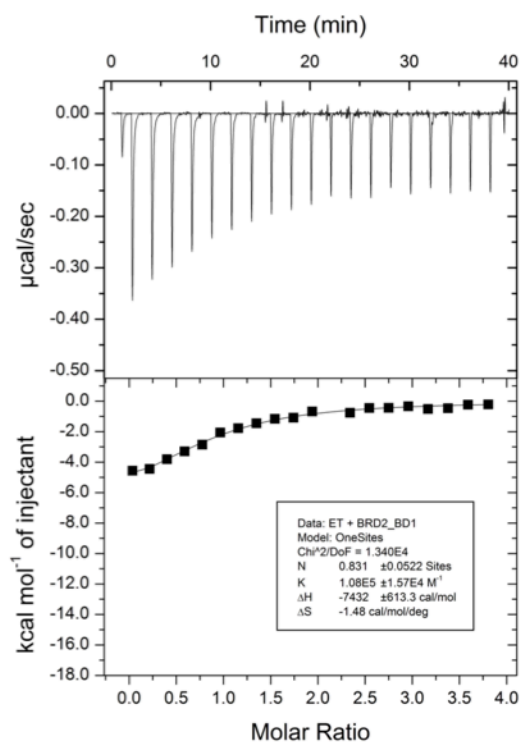


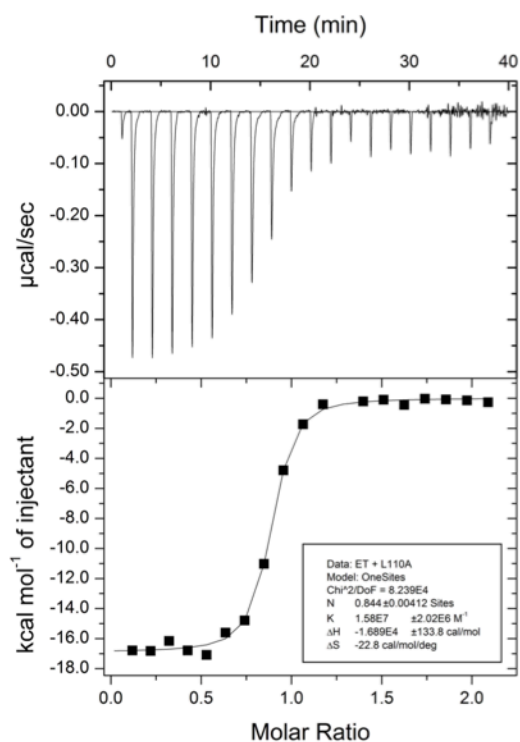
**Fig. S8.**

X-ray crystal structures show retention of ligand binding mode and support the bump-and-hole design strategy. Ethyl functionalized I-BET analogue **ET** (sticks, purple carbons) bound to brd2(2) L383A mutant (green surface, A383 shown as sticks with green carbons) is shown superimposed with (A) I-BET bound to brd2(1) WT (pdb 2YEK (4), I-BET shown as sticks, yellow carbons) and with (B) JQ1 bound to brd2(2) WT (pdb 3ONI (3), JQ1 shown as sticks, cyan carbons). (C) Methyl and ethyl functionalized analogues **ME** and **ET** exhibit identical binding modes to brd2(2) L383A (light green surface, key residues at the KAc binding site shown as ball-and-sticks and labelled). (D) The ethyl bump of **ET** achieves the desired steric clash with the side chain of Leu383 (shown as sticks, cyan carbons) present in brd2(2) WT (pdb 3ONI (3), protein shown as deep teal surface, ligand JQ1 omitted for clarity).

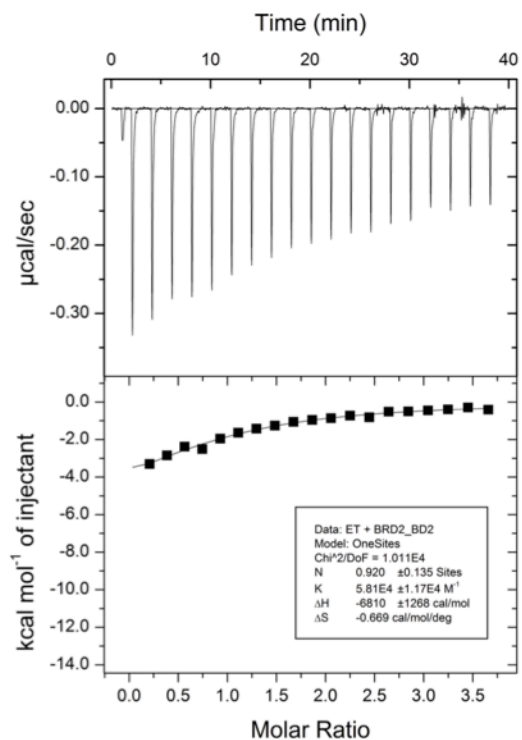
A)



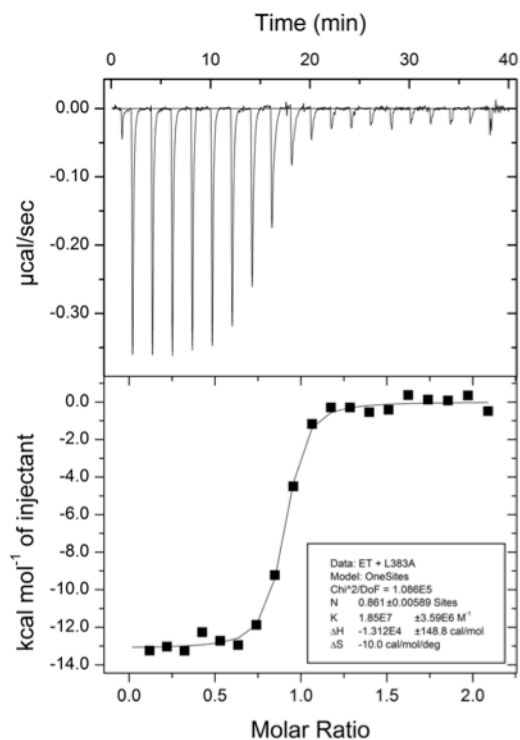
B)



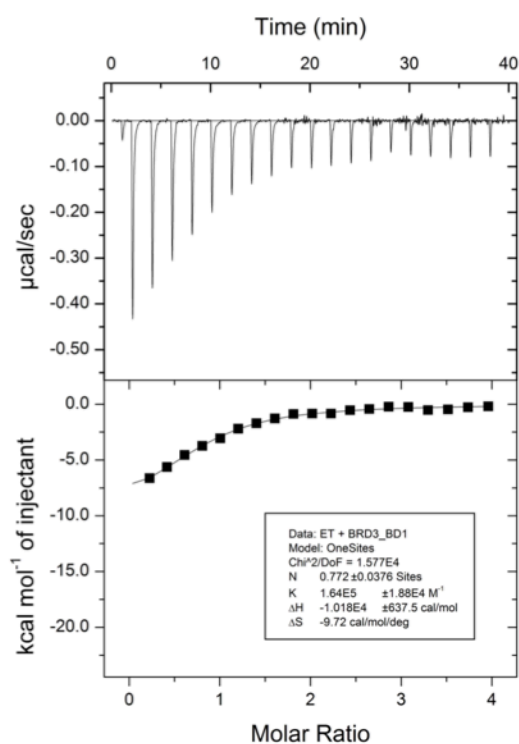
C)



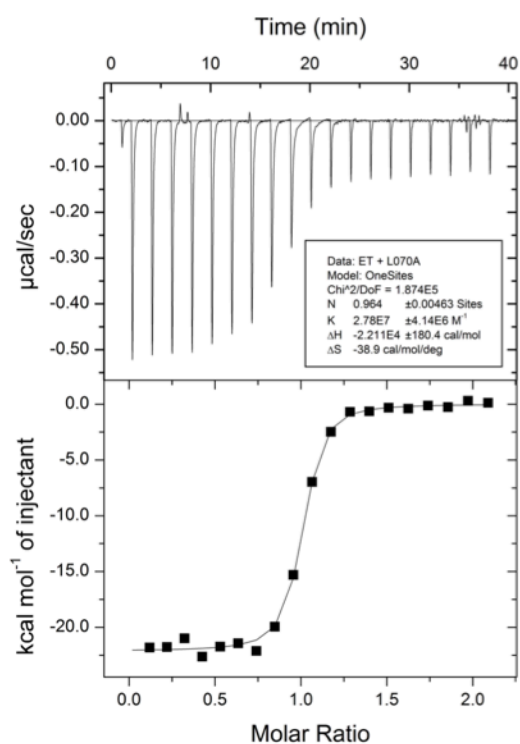
D)



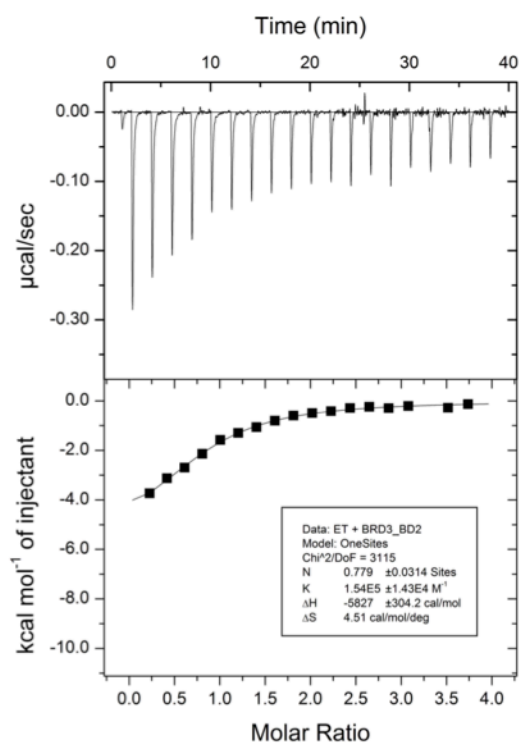
E)



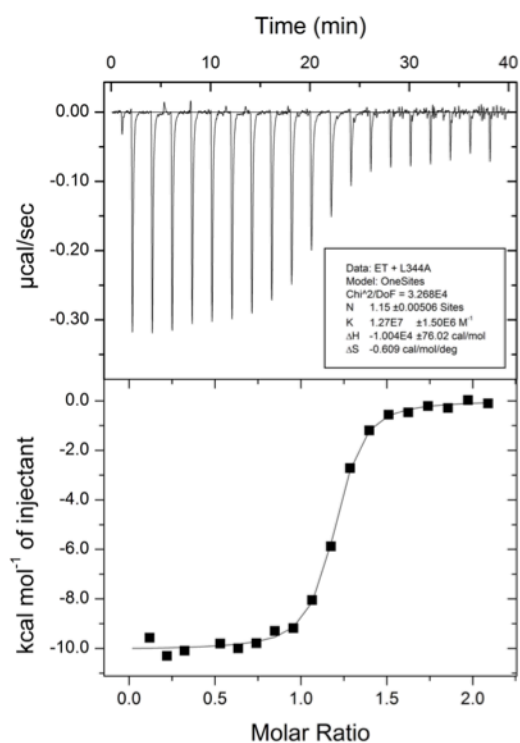
F)



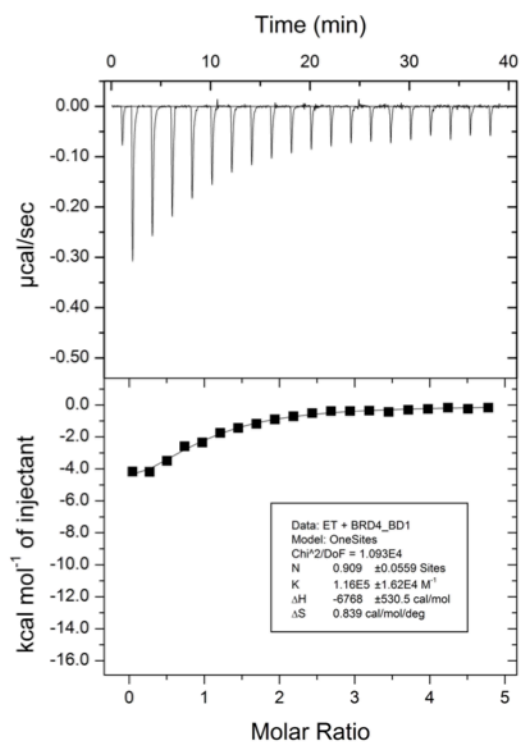
G)



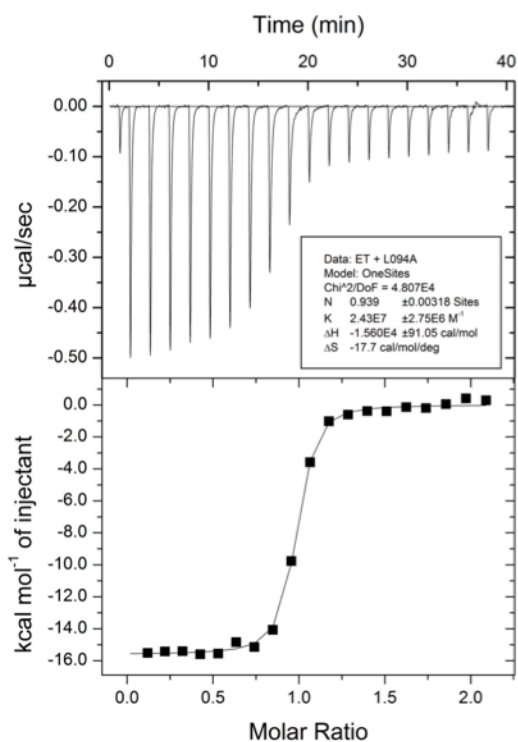
H)



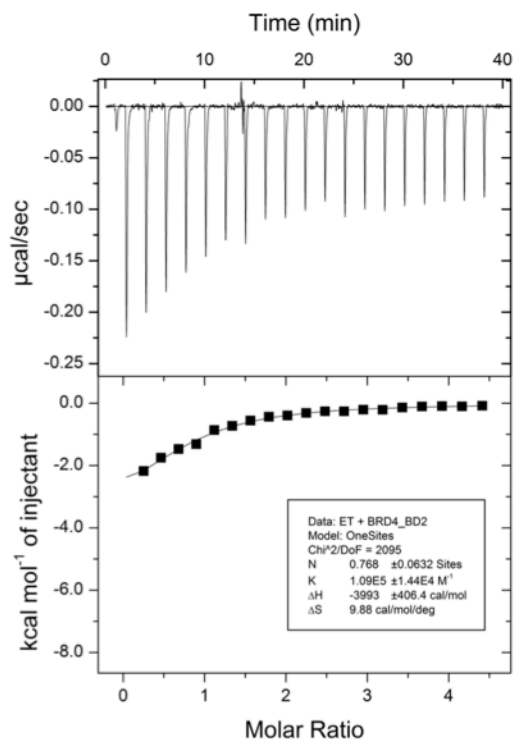
I)



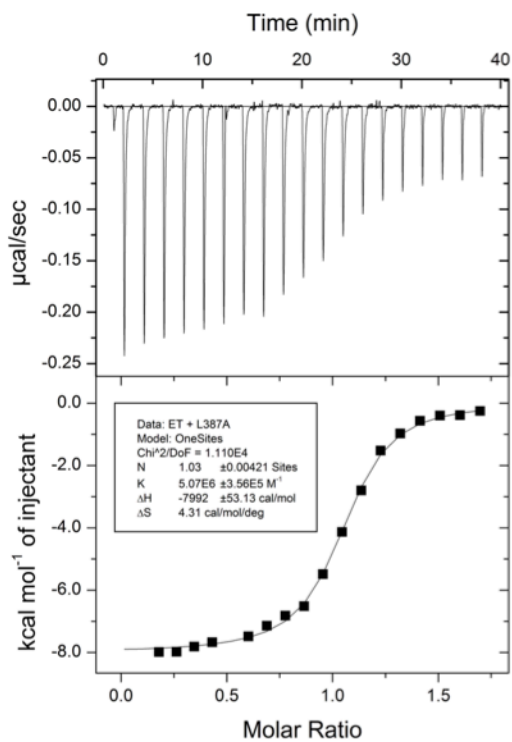
J)



K)



L)





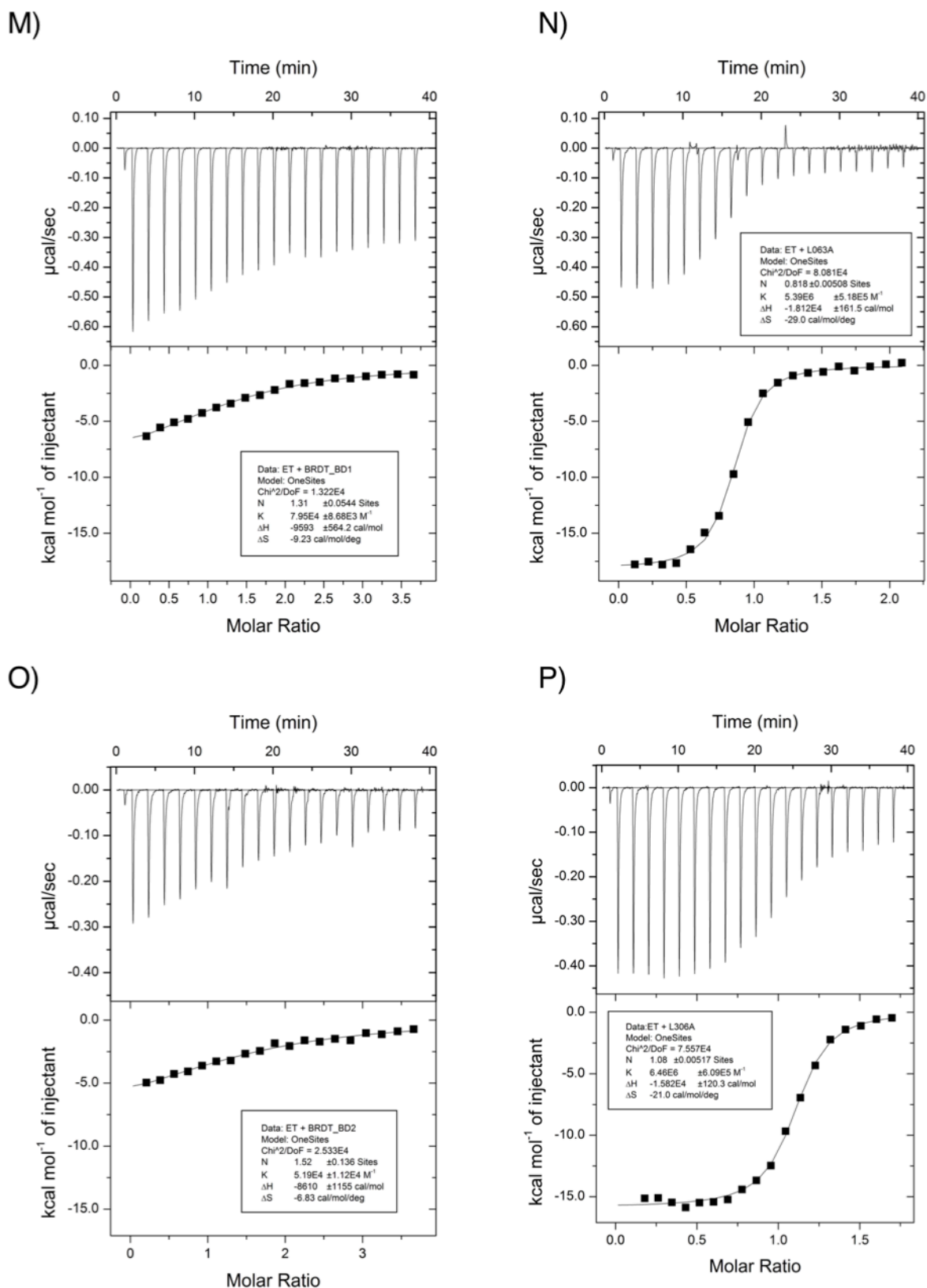


**Fig. S9.**

ITC titration curves of WT and L/A mutants of BET bromodomains binding to ET. A-B) brd2(1); C-D) brd2(2); E-F) brd3(1); G-H) brd3(2); I-J) brd4(1); K-L) brd4(2); M-N) brdt(1); O-P) brdt(2). Conditions: reverse titrations at 30 °C of WT (350-400 µM) into ET (20 µM) and L/A mutants (110-150 µM) into ET (10-15 µM).

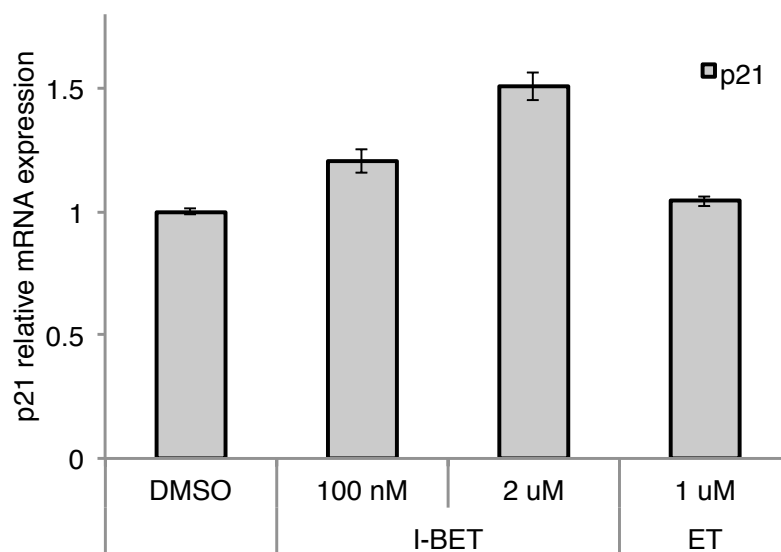
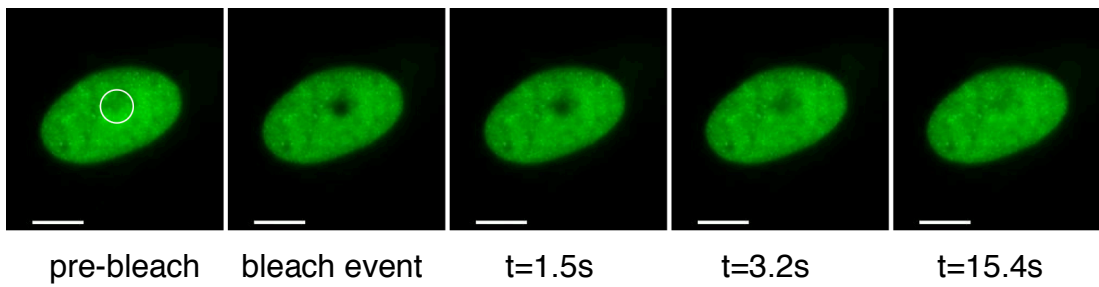


**Fig. S10.**

Pharmacological up-regulation of p21 mRNA levels is achieved with I-BET but not with **ET**. U2OS cells were treated with either I-BET or **ET** for 6h and p21 mRNA expression level was monitored by qPCR as a report of pharmacological inhibition of WT BET bromodomain function. I-BET treatment led to increased expression levels of p21 at 0.1 and 2  $\mu$ M as previously reported (14) while **ET** did not induce such effect at 1  $\mu$ M concentration, confirming its inactivity against WT bromodomains. The data shown represent the mean  $\pm$  standard deviations of three measurements.

A)



B)

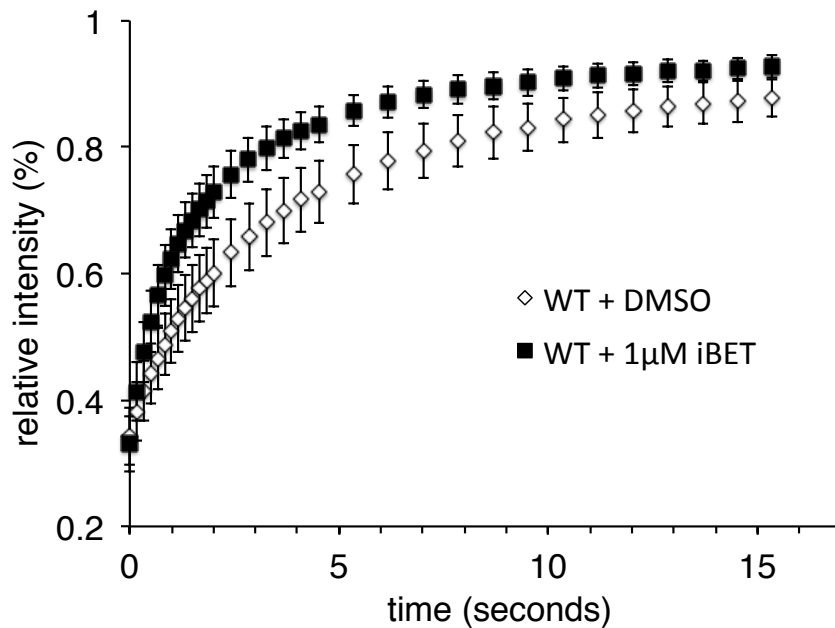


**Fig. S11.**

Fluorescence recovery after photobleaching (FRAP) evaluation of human GFP-brd4 dissociation from chromatin. A) Images are shown at different time points for a representative nucleus of U2OS cells transfected with wild-type GFP-brd4 and treated with 1  $\mu$ M of compound **ET**. The target region of photobleaching is indicated by a white circle. Scale bars: 10  $\mu$ m region. B) Representative time-dependence profiles of the fluorescence recovery of U2OS cells nuclei treated with DMSO vehicle (white diamonds) or 1  $\mu$ M I-BET (black squares). The data shown represent the mean  $\pm$  standard deviations (n = 40 for DMSO treatment, n = 50 for I-BET treatment).

**Table S1.**

Thermodynamic parameters measured by isothermal titration calorimetry (ITC) for the binding of I-BET to BET bromodomains. Conditions: reverse titrations of WT BET bromodomains (150  $\mu$ M) into I-BET (15  $\mu$ M) at 25°C.

brd	N	K <sub>d</sub> (nM)	$\Delta$ G (cal/mol)	$\Delta$ H (cal/mol)	$\Delta$ S (cal/mol/K)
<b>brd2(1)</b>	0.84 $\pm$ 0.01	230 $\pm$ 20	-9060 $\pm$ 60	-14800 $\pm$ 140	-19.3 $\pm$ 0.5
<b>brd2(2)</b>	0.89 $\pm$ 0.01	100 $\pm$ 10	-9550 $\pm$ 70	-11000 $\pm$ 90	-4.9 $\pm$ 0.4
<b>brd3(1)</b>	1.08 $\pm$ 0.01	70 $\pm$ 10	-9780 $\pm$ 80	-14200 $\pm$ 110	-15.0 $\pm$ 0.5
<b>brd3(2)</b>	1.02 $\pm$ 0.01	54 $\pm$ 4	-9930 $\pm$ 50	-13200 $\pm$ 60	-10.9 $\pm$ 0.3
<b>brd4(1)</b>	0.91 $\pm$ 0.01	95 $\pm$ 10	-9590 $\pm$ 60	-11700 $\pm$ 80	-7.1 $\pm$ 0.3
<b>brd4(2)</b>	1.09 $\pm$ 0.01	65 $\pm$ 15	-9820 $\pm$ 130	-11000 $\pm$ 140	-3.9 $\pm$ 0.6
<b>brdt(1)</b>	1.06 $\pm$ 0.01	340 $\pm$ 50	-8830 $\pm$ 90	-16200 $\pm$ 250	-24.6 $\pm$ 0.9
<b>brdt(2)</b>	1.03 $\pm$ 0.01	370 $\pm$ 40	-8780 $\pm$ 60	-13330 $\pm$ 140	-15.3 $\pm$ 0.5

**Table S2.**

Biophysical characterization of WT and L/A mutant BET bromodomains. Melting temperature ( $T_m$ ) and variation of  $T_m$  compared to the respective wild type ( $\Delta T_m$ ). WT and mutant proteins (2  $\mu$ M) were submitted to a temperature ramp from 37 °C to 95 °C.

brd	$T_m$ (°C)	$\Delta T_m$ from WT
<b>brd2(1)</b>	46.2 $\pm$ 0.2	/
<b>brd2(2)</b>	47.5 $\pm$ 0.1	/
<b>brd3(1)</b>	46.4 $\pm$ 0.1	/
<b>brd3(2)</b>	41.5 $\pm$ 0.6	/
<b>brd4(1)</b>	44.6 $\pm$ 0.2	/
<b>brd4(2)</b>	44.7 $\pm$ 0.0	/
<b>brdt(1)</b>	48.6 $\pm$ 0.1	/
<b>brdt(2)</b>	44.4 $\pm$ 0.2	/
<b>brd2(1)<sub>L110A</sub></b>	43.7 $\pm$ 0.0	-2.5 $\pm$ 0.2
<b>brd2(2)<sub>L383A</sub></b>	44.8 $\pm$ 0.1	-2.7 $\pm$ 0.2
<b>brd3(1)<sub>L070A</sub></b>	44.8 $\pm$ 0.1	-1.6 $\pm$ 0.2
<b>brd3(2)<sub>L344A</sub></b>	40.5 $\pm$ 0.1	-1.0 $\pm$ 0.7
<b>brd4(1)<sub>L094A</sub></b>	44.8 $\pm$ 0.1	0.2 $\pm$ 0.3
<b>brd4(2)<sub>L387A</sub></b>	44.8 $\pm$ 0.1	0.1 $\pm$ 0.1
<b>brdt(1)<sub>L063A</sub></b>	47.4 $\pm$ 0.2	-1.2 $\pm$ 0.3
<b>brdt(2)<sub>L306A</sub></b>	45.3 $\pm$ 0.2	0.9 $\pm$ 0.4

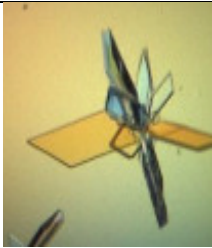
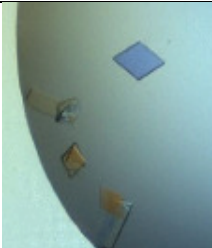
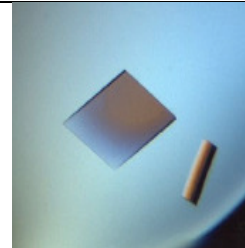
**Table S3.**

Biophysical characterization of the binding of a tetra-acetylated H4 derived peptide to WT and LA mutant of BET bromodomains. ITC data are from titrations of peptide (1-4 mM) into WT and LA mutant proteins (50-100  $\mu$ M) of single bromodomains of brd2 and brd4, and tandem bromodomain constructs (80-100  $\mu$ M) of brd2 at 15°C.

H <sub>2</sub> N-YSGRGK(Ac)GGK(Ac)GLGK(Ac)GGAK(Ac)RHRK-COOH				
brd	$K_d$ ( $\mu$ M)	$\Delta G$ (cal/mol)	$\Delta H$ (cal/mol)	$\Delta S$ (cal/mol/°)
<b>brd2(1)</b>	26.5 $\pm$ 1.4	-6040 $\pm$ 30	-14800 $\pm$ 350	-30.3 $\pm$ 1.2
<b>brd2(1)<sub>L110A</sub></b>	121 $\pm$ 5	-5170 $\pm$ 20	-6240 $\pm$ 240	-3.7 $\pm$ 0.8
<b>brd2(2)</b>	77.0 $\pm$ 7.5	-5430 $\pm$ 60	-4600 $\pm$ 400	3.0 $\pm$ 1.4
<b>brd2(2)<sub>L383A</sub></b>	120 $\pm$ 8	-5180 $\pm$ 40	-2700 $\pm$ 200	8.5 $\pm$ 0.6
<b>brd4(1)</b>	10.1 $\pm$ 0.5	-6590 $\pm$ 30	-11700 $\pm$ 100	-17.7 $\pm$ 0.4
<b>brd4(1)<sub>L094A</sub></b>	94 $\pm$ 3	-5310 $\pm$ 20	-12800 $\pm$ 700	-26.0 $\pm$ 2.4
<b>brd4(2)</b>	156 $\pm$ 7	-5020 $\pm$ 30	-4900 $\pm$ 200	0.4 $\pm$ 0.7
<b>brd4(2)<sub>L387A</sub></b>	48 $\pm$ 4	-5690 $\pm$ 50	-2700 $\pm$ 300	10.5 $\pm$ 0.9
<b>brd2 (wt-wt)</b>	20.0 $\pm$ 2.0	-6202 $\pm$ 60	-14600 $\pm$ 400	-29.1 $\pm$ 1.6
<b>brd2 (LA-wt)</b>	100.0 $\pm$ 6.5	-5280 $\pm$ 40	-6400 $\pm$ 530	-3.9 $\pm$ 1.8
<b>brd2 (wt-LA)</b>	18.7 $\pm$ 0.7	-6240 $\pm$ 20	-11700 $\pm$ 140	-18.9 $\pm$ 0.5
<b>brd2 (LA-LA)</b>	152 $\pm$ 17	-5040 $\pm$ 60	-6600 $\pm$ 700	-5.6 $\pm$ 2.4

**Table S4.**

X-ray crystallography: data collection and refinement statistics.

PROTEIN ID PDB ID	Brd2(2)-L383A 4QEU	Brd2(2)-L383A 4QEV	Brd2(2)-L383A 4QEW
<b>Data collection</b>			
Space Group	C2	P2 <sub>1</sub> 2 <sub>1</sub> 2	P2 <sub>1</sub> 2 <sub>1</sub> 2
Cell Dimensions			
a,b,c (Å)	82.51 35.21	52.52 71.47 32.07	52.38 71.03 31.98
α, β, γ (deg)	48.49	90.00 90.00	90.00 90.00 90.00
	90.00 118.82	90.00	
	90.00		
Resolution (Å)	38.0 (1.50) <sup>a</sup>	32.1 (1.80) <sup>a</sup>	42.2 (1.70) <sup>a</sup>
Unique	19862 (3548)	11758 (1730)	13733 (2103)
Observations			
Completeness (%)	99.6 (98.0)	99.4 (96.6)	99.9 (99.6)
Redundancy	5.6 (3.2)	6.4 (4.1)	6.2 (3.9)
<i>R</i> <sub>sym</sub> or <i>R</i> <sub>merge</sub>	0.062 (0.383)	0.110 (0.437)	0.077 (0.377)
<i>I</i> / <i>σI</i>	16.1 (3.1)	11.3 (3.3)	15.2 (3.0)
Wavelength	1,5418	1,5418	1,5418
<b>Refinement</b>			
<i>R</i> <sub>work</sub> / <i>R</i> <sub>free</sub> (%)	16.2 / 18.9	18.7 / 22.6	17.7 / 21.0
Number of atoms			
	935 / 10 / 123	920 / 59 / 69	943 / 61 / 66
protein/other/solvent			
B-Factors (Å <sup>2</sup> )			
	12.81 / 12.41 /	9.89 / 31.40 /	11.88 / 25.34 /
protein/other/solvent	22.63	18.94	21.00
R.M.S.D. Bond (Å)	0.014	0.009	0.010
R.M.S.D. Angle (°)	1.513	1.479	1.525
Ramachandran			
statistics:	100.00	100.00	100.00
Allowed (%)	100.00	99.07	99.09
Favored (%)	0.00	0.00	0.00
Outliers (%)			
Ligand	-	ME	ET
			
<sup>a</sup> Highest resolution shell (in Å) shown in parentheses.			

**Table S5.**

Thermal stabilization ( $\Delta T_m$ ) and thermodynamic binding parameters for **ET** against WT and L/A mutants of the eight BET bromodomains, as measured by DSF and ITC at 30 °C, respectively.

brd	$\Delta T_m$ (°C)	$N$	$K_d$ (nM)	$\Delta G$ (cal/mol)	$\Delta H$ (cal/mol)	$\Delta S$ (cal/mol/K)
<b>brd2(1)</b>	$1.2 \pm 0.2$	$0.83 \pm 0.05$	$9300 \pm 1350$	$-6990 \pm 90$	$-7430 \pm 610$	$-1.5 \pm 2.0$
<b>brd2(2)</b>	$1.6 \pm 0.1$	$0.92 \pm 0.13$	$17200 \pm 3500$	$-6600 \pm 120$	$-6810 \pm 1270$	$-0.6 \pm 4.2$
<b>brd3(1)</b>	$2.2 \pm 0.1$	$0.77 \pm 0.04$	$6100 \pm 700$	$-7240 \pm 70$	$-10200 \pm 640$	$-9.7 \pm 2.1$
<b>brd3(2)</b>	$2.6 \pm 0.7$	$0.78 \pm 0.03$	$6500 \pm 600$	$-7200 \pm 60$	$-5830 \pm 300$	$4.5 \pm 1.0$
<b>brd4(1)</b>	$1.5 \pm 0.4$	$0.91 \pm 0.06$	$8600 \pm 1200$	$-7030 \pm 80$	$-6770 \pm 530$	$0.8 \pm 1.8$
<b>brd4(2)</b>	$1.5 \pm 0.0$	$0.77 \pm 0.06$	$9200 \pm 1200$	$-6990 \pm 80$	$-4000 \pm 400$	$9.9 \pm 1.4$
<b>brdt(1)</b>	$1.5 \pm 0.4$	$1.31 \pm 0.05$	$12600 \pm 1400$	$-6800 \pm 70$	$-9600 \pm 600$	$-9.2 \pm 1.9$
<b>brdt(2)</b>	$1.3 \pm 0.3$	$1.52 \pm 0.01$	$19300 \pm 4200$	$-6550 \pm 130$	$-8600 \pm 1150$	$-6.8 \pm 3.8$
<b>brd2(1)<sub>L110A</sub></b>	$7.6 \pm 0.2$	$0.84 \pm 0.01$	$63 \pm 8$	$-9990 \pm 80$	$-16900 \pm 130$	$-22.7 \pm 0.5$
<b>brd2(2)<sub>L383A</sub></b>	$8.1 \pm 0.2$	$0.86 \pm 0.01$	$54 \pm 10$	$-10090 \pm 120$	$-13100 \pm 150$	$-10.0 \pm 0.6$
<b>brd3(1)<sub>L070A</sub></b>	$10.4 \pm 0.3$	$0.96 \pm 0.01$	$36 \pm 5$	$-10330 \pm 90$	$-22100 \pm 180$	$-38.8 \pm 0.7$
<b>brd3(2)<sub>L344A</sub></b>	$13.4 \pm 0.6$	$1.15 \pm 0.01$	$79 \pm 9$	$-9860 \pm 70$	$-10000 \pm 80$	$-0.6 \pm 0.3$
<b>brd4(1)<sub>L094A</sub></b>	$10.0 \pm 0.2$	$0.94 \pm 0.01$	$41 \pm 5$	$-10250 \pm 70$	$-15600 \pm 90$	$-17.6 \pm 0.4$
<b>brd4(2)<sub>L387A</sub></b>	$7.0 \pm 0.1$	$1.03 \pm 0.01$	$197 \pm 14$	$-9310 \pm 450$	$-8000 \pm 50$	$4.3 \pm 0.2$
<b>brdt(1)<sub>L063A</sub></b>	$5.4 \pm 0.3$	$0.82 \pm 0.01$	$186 \pm 18$	$-9350 \pm 60$	$-18100 \pm 160$	$-28.9 \pm 0.6$
<b>brdt(2)<sub>L306A</sub></b>	$6.7 \pm 0.4$	$1.08 \pm 0.01$	$155 \pm 15$	$-9460 \pm 60$	$-15800 \pm 120$	$-21.0 \pm 0.4$



**Table S6.**

Binding selectivity profile of **ET** against WT and engineered BET bromodomain mutants. The selectivity factors are defined by the ratio  $K_a(L/A)/K_a(WT)$ . E.g. **ET** is 223 fold more potent against  $\text{brd4(1)}_{L094A}$  than against WT  $\text{brd4(2)}$ .

brd	<b>brd2(1)</b>	<b>brd2(2)</b>	<b>brd3(1)</b>	<b>brd3(2)</b>	<b>brd4(1)</b>	<b>brd4(2)</b>	<b>brdt(1)</b>	<b>brdt(2)</b>
<b>brd2(1)</b> <sub>L110A</sub>	146	272	96	103	136	145	199	304
<b>brd2(2)</b> <sub>L383A</sub>	171	318	113	120	159	170	233	356
<b>brd3(1)</b> <sub>L070A</sub>	257	478	170	181	240	255	350	536
<b>brd3(2)</b> <sub>L344A</sub>	118	219	77	82	109	117	160	245
<b>brd4(1)</b> <sub>L094A</sub>	225	418	148	158	209	223	306	468
<b>brd4(2)</b> <sub>L387A</sub>	47	87	31	33	44	47	64	98
<b>brdt(1)</b> <sub>L063A</sub>	50	93	33	35	46	49	68	104
<b>brdt(2)</b> <sub>L306A</sub>	60	111	39	42	56	59	81	124